8-9-2021

Determination and Comparison of the Effects of Nitrogen and Sulfur Deprivations on Chlamydomonas ReinhardtII Strain CC5373-STAG

David Gonzalez

DETERMINATION AND COMPARISON OF THE EFFECTS OF NITROGEN AND SULFUR DEPRIVATIONS ON CHLAMYDOMONAS REINHARDTII STRAIN CC5373-STA6

A Thesis

by

DAVID GONZALEZ

Submitted to Texas A&M International University
in partial fulfillment of the requirements
for the degree of

MASTER OF SCIENCE

August 2021

Major Subject: Biology

DETERMINATION AND COMPARISON OF THE EFFECTS OF NITROGEN AND SULFUR DEPRIVATIONS ON CHLAMYDOMONAS REINHARDTII STRAIN CC5373-STA6

A Thesis

by

DAVID GONZALEZ

Submitted to Texas A&M International University
in partial fulfillment of the requirements
for the degree of

MASTER OF SCIENCE

Approved as to style and content by:

Chair of Committee,	Ruby A. Ynalvez
Committee Members,	Cord Eversole
	Monica O. Mendez
	Yang Lee
Head of Department,	Michael R. Kidd

August 2021

Major Subject: Biology

ABSTRACT

The use of microalgae in biodiesel production is of increasing interest due to the capability of enhancing the algae's triacylglycerol (TAG) biosynthesis by the use of stress conditions to optimize microalgal TAG accumulation. Nitrogen starvation causes algal cells to accumulate starch and increase lipid content; sulfur deprivation increases H_2 production and increases lipid content. *Chlamydomonas reinhardtii* starchless mutant cc5373-sta6, which due to an inhibited starch biosynthesis has greater accumulation of lipid bodies. To our knowledge, no studies yet have reported a combined nitrogen (N) and sulfur (S) deprivation as a stress condition for lipid production and using the starchless mutant, cc5373-sta6. We hypothesized that by removing both N and S from cc5373-sta6's growth media, lipid bodies will over accumulate within the cell, greater than when solely using N or S deprivation. The purpose of this study was to compare the effects of nutrient deprivation conditions on cc5373-sta6 via chemical, microscopic and genetic analysis. The objectives of this study were to (1) determine the effects of nitrogen and sulfur starvation on cc5373-sta6 by conducting spectrophotometric analyses (cell density, chlorophyll content and biomass determination), (2) determine lipid accumulation via confocal microscopy and (3) identify the transcriptional expression levels of enzymes involved in lipid biosynthesis by RT-PCR. Chemical analyses for nutrient deprived cells displayed significant increase in cell density ($p<0.001$) and a significant decrease in chlorophyll content ($p<0.001$). Confocal imaging showed N and S deprived cells to accumulate large lipid bodies. More specifically, after 48 hr NS deprived cells showed significantly larger lipid body size ($p<0.001$). Cells subjected to N and S deprivation increased expression of ACCase after 8 hr and 24 hr ($p<0.001$); PEPC expression decreased after 8 hr, and increased after 24 hr ($p<0.001$). This study is the first to report the combinatorial effects of N and S deprivation have on lipid accumulation in cc5373-sta6. In addition, the results of this study will serve as a basis for further studies on the potential of *C. reinhardtii* cc-5373-sta6 for biofuel production.

ACKNOWLEDGEMENTS

The research presented in this manuscript could not have been completed without the outstanding mentorship of Dr. Ruby A. Ynalvez (chair), Dr. Cord B. Eversole, Dr. Monica Mendez, and Dr. Yang Lee. The guidance this graduate committee offered was instrumental to the progression of this research and should be worth mentioning. A special thank you to Dr. Marcus Ynalvez for assistance and mentorship in experimental design and statistical analysis. Acknowledgment to the National Science Foundation Major Research Instrumentation Award ##1726888 for the confocal microscope.

TABLE OF CONTENTS

LIST OF FIGURES

LIST OF TABLES

1 INTRODUCTION

1.1 Background of the study

It has been a challenge to develop renewable energy sources without diminishing the quality of the environment. As global growth increases it is inevitable for the availability of fossil fuels to decrease, resulting in rising energy prices worldwide (Scranton et al., 2015). As the cost of energy increases so too does the cost of food; thus, there is a need to find alternative sources of renewable energy that do not compromise the quality of the environment. Recently, the use of microalgae in biodiesel production has received considerable attention as a great option as a renewable energy source. Microalgae have many advantages over crop and land plants due to their sustainability. Microalgae are easier to grow, have a higher productivity, and can be grown in unfavorable conditions (Potijun et al., 2020). However, limitations at the technological level such as cultivation methods, lipid extraction, and cost of growing, have made it unsuitable for industrial production. A primary option to facilitate the commercialization of microalgae is to improve triacylglycerol (TAG) production in the microalgae (Potijun et al., 2020).

Chlamydomonas reinhardtii offers advantages for biofuel production research. This is due to its extensive genetic characterization. Likewise, *C. reinhardtii* has received increasing interest because of its ability to enhance the algae's triacylglycerol biosynthesis (Zabawinski et al., 2001; Cakmak et al., 2012; Cakmak et al., 2015; Tran et al., 2019). *C. reinhardtii* has the ability to synthesize and accumulate significant quantities of lipids in the form of triacyclglycerols (TAGs) under specific stress conditions. Studies have shown that stresses such as light intensity alterations, nutrient deprivation, and the addition of salts cause an influx of TAGs to be produced in the cell (Cakmak et al., 2012; Cakmak et al., 2015; Gargouri et al., 2017; Xhu et al., 2018; Zhu et al, 2021). Specifically, nitrogen (N) starvation elicits a differentiation of algal cells into gametes, an accumulation of carbohydrates, an increase in TAG content and an autophagy response (Cakmak et al., 2015; Salas-Montantes et al., 2018; Sathe et al., 2019). Research on *C. reinhardtii*

This thesis follows the model of *Biotechnology and Bioengineering*.

also indicates that sulfur (S) deprivation causes an inactivation of photosynthetic activity, an increase of H_2 production, and an increase in lipid content in the form of TAGs (Cakmak et al., 2012; Grechanik et al., 2020). Studies indicate that depriving the microalgae of N and S after four days has resulted in a significant amount of lipids in the form of TAG accumulation (Cakmak et al., 2012; Cakmak et al., 2015). To our knowledge, there have been no studies reported yet on how the combination of nitrogen and sulfur deprivation affects the cell growth, chlorophyll content and TAG biosynthesis in *C. reinhardtii*.

To further industrialize *C. reinhardtii* as a source for biofuel production, it is important to consider the growth and energy storage compounds accumulated in the strain used. It is known that alterations made to cellular metabolic pathways via genetic modifications in microalgae can enhance or reduce specific metabolite production (Tran et al., 2019). Mutants from the wild-type strain of *C. reinhardtii* have become of interest due to their capability of enhancing lipid bodies during development. Specifically, the starchless mutant cc5373-sta6 has been used in research due to the inhibition in the subunit of the regulatory enzyme responsible for starch biosynthesis, ADP-glucose pyrophosphorylase (Zabawinski et al., 2001). By inhibiting the production of specific energy storage compounds, this strain facilitates the increase in other storage compounds, such as lipids. The sta6 strain has been shown to increase TAG content by 10-fold as compared to the wild type via nutrient deprivation conditions (Goodenough et al., 2014; Tran et al., 2019; Shin et al., 2018). Although lipid production has been already studied in this strain, there is still a need to further characterize the strain and optimize its cultivation conditions before it is offered commercially. By utilizing stress conditions and with the use of *C. reinhardtii* mutants, the microalgae can be a good potential alternative renewable source of energy.

The purpose of this study is to compare the effects of nitrogen (N), sulfur (S) and the combination of nitrogen and sulfur deprivations on cc5373-sta6 via chemical, microscopic and genetic analysis and to establish optimal conditions for lipid bodies (TAG) biosynthesis in *C. reinhardtii*. The central hypothesis is: the removal of N and S in Tris-acetate-phosphate (TAP) growth media will increase lipid biosynthesis in the starchless mutant of *C. reinhardtii,* cc5373-sta6. The objectives of this study are to (1) determine the effects of N and S starvation on cc5373-sta6's growth by conducting chemical analysis (cell density,

chlorophyll content analysis, and biomass determination), (2) quantify lipid body accumulation (TAG) via confocal microscopy imaging analysis and (3) identify the transcriptional expression levels of the enzymes involved in lipid biosynthesis, acetyl-CoA carboxylase (ACCase) and phosphoenolpyruvate carboxylase (PEPC), by RT-PCR. This study will contribute to the scientific knowledge on (1) cc5373-sta6's potential as a renewable source of energy and (2) the commercialization of microalgae by improving triacylglycerol (TAG) production in the microalgae. Although there is a larger volume of literature on the microalgae's starch biosynthesis, there is less documented literature on its lipid biosynthesis. Thus, the results of this research will be a relevant addition to the knowledge on microalgae's lipid biosynthesis.

1.2 Review of literature

Fossil fuel use and environmental effects. The burning of fossil fuels has been the primary form of energy to fuel daily human activities. With the increase in population and the growing economy, the demand for fossil fuels is projected to increase exponentially (Piggot et al., 2020). Fossil fuels are derived from organic materials of plants and animals that have been fossilized over time. The most common types of fossils are coal, crude oil and natural gas, whereby coal accounts for approximately 25% of energy consumption and 40% of the electricity generated globally (Smith et al., 2013). Although fossil fuels have improved the quality of life, global warming and pollution have negatively impacted our environment. The accumulation of greenhouse gases, such as carbon dioxide, methane, and nitrous oxide, prevents heat from leaving the atmosphere allowing for a gradual increase in overall global temperature. Extensive research has indicated that industrial processes, such as burning of fossil fuels, have contributed to a major proportion of greenhouse emission of CO_2 (Wuebbles & Jain, 2001; Jain, 2019). Aside from carbon dioxide emissions, methane emissions, petroleum oil spills, and water contamination as a result of anthropogenic activities are of great concern to the environment and human health. The use of novel, sustainable, and renewable sources of energy without sacrificing the quality of the environment is more prevalent than ever (Erickson et al., 2018; Piggot et al., 2020).

Alternative renewable sources of energy. Biofuels are a preferred alternative source of energy. They are energy-rich chemicals that are naturally generated through biological processes (Rodionova et al., 2017). There are three major groups of biofuels: first generation, second generation, and third generation (Aro, 2016). First generation biofuels are sourced from crop plants as energy-containing molecules like sugars, oils and cellulose; they provide a limited amount of biofuel production (Aro, 2016). Second generation biofuels are produced from the feedstock of lignocellulosic, non-food materials that include straw, bagasse, and forest residues. These types of biofuels have yet to become maximized to achieve a substantial amount of carbon and hydrogen that can be converted to fuels (Aro, 2016). Third generation biofuels are based on algal biomass production and are under constant extensive research. The objective of third generation biofuels is to enhance the metabolic production of fuels and to separate the processes of bio-oil production to remove non-fuel components to lower production cost (Aro, 2016). There is an issue with utilizing algal species as biodiesel production; biofuel production only occurs during stress conditions that reduce the growth and biomass production of the organism. However, there have been significant advancements in metabolic engineering of algae to increase lipids without compromising growth resulting in sustainable biodiesel production (Trentacoste et al., 2013, Xu et al., 2018).

Algae for biofuel production. Microalgae are designated as the primary converters of CO_2/O_2; they offer many valuable products such as pigments, vitamins, and biofuel feedstock. Algae are used in wastewater treatment, production of protein rich food and feed additives, and biofuel (Demirbas, 2008; Doan et al., 2011). As aforementioned, there is an increasing need for renewable energy sources, specifically biofuels, due to the limited fossil fuel reserves. The use of microalgae has provided a promising third generation biofuel source, but to better enhance the utilization of microalgae as a source of biofuel, knowledge on increasing biofuel feedstock must be improved (Moazami et al., 2011). For instance, increasing products such as triacyclglycerol (TAG) and biohydrogen in microalgae provide a good energy source for biofuel production (Xu et al., 2018; Xu et al., 2019).

The process of TAG synthesis is essential in an organism. TAGs are the major constituents of vegetable oil, algal lipid bodies, and animal fats (Cakmak et al., 2012). A TAG consists of an ester of three fatty acids and a glycerol backbone that is synthesized by almost all eukaryotic organisms. In biodiesel production TAGs can be used directly or they can be transesterified producing a fatty acid methyl ester. In addition, the glycerol backbone can also be utilized by being converted into ethanol. If the market for biodiesel increases, there is a need to focus on glycerol metabolism to increase cost effectiveness and to avoid accumulation of reduced carbon waste products (Merchant, et al., 2012). Although the process of converting carbohydrates to ethanol is well-developed, there are greater advantages using oils, specifically TAGs. For instance, the net energy balance for biodiesel from oil is 93% and it releases only a fraction of the pollutants on a per net energy gain basis relative to that of ethanol (Merchant, et al., 2012).

Although the biomass of land plants can be converted to lignocellulosic-derived alcohols, there are major disadvantages to utilizing them. Arable land used for biofuel production from crop plants compensates food supplies, impacts opportunity cost with respect to land use for housing and other uses for the population and has a negative long-term environmental impact (Merchant et al., 2012). Thus, the TAGs accumulated in microalgae have received much attention for their potential as biodiesel producers. One of the major advantages of using microalgae for biofuel production is that they can be grown in wastewater relying strongly on their photosynthetic productivity. Algae can also be grown in closed photobioreactors or in open raceways that further establishes its usefulness towards commercial operations. The goal of algal biofuel research is to identify species that will become biofuel "crops", understand the metabolic pathways that contribute to TAG synthesis, and establish the regulatory events that initiate TAG accumulation in response to stress. Thus, due to its extensive genetic characterization, researchers typically utilize the model green algae, *Chlamydomonas reinhardtii,* to meet the algal biofuel research goals.

C. reinhardtii as a model for biofuel production. C. reinhardtii, is an alga typically used in studying lipid metabolism via nutrient stress (Ball et al., 1998; Moellering and Benning, 2010; Xu et al., 2018; Shin et al., 2019). *Chlamydomonas* research is typically geared towards understanding algal metabolism,

particularly in carbon metabolism and photosynthesis. Thus, it serves as an excellent model organism to understand and improve biofuels and bio-product production in algae (Scranton et al. 2015; Li-Beisson et al., 2015). *C. reinhardtii* has led the field in development of molecular tools for strain selection and engineering for green alga (Scranton et al., 2015). To date, more recombinant proteins have been expressed in *C. reinhardtii* than any other algal species (Rasala and Mayfield, 2014; Scranton et al., 2015).

C. reinhardtii has also elucidated molecular mechanisms in algal lipid and hydrogen metabolism that has allowed *C. reinhardtii* to become the first engineered algal species to be studied in commercial settings. As an alternative to liquid fuels, *C. reinhardtii* has been studied as a model for photoproduction of biohydrogen (Scranton et al., 2015). Under sulfur deprived conditions, biohydrogen production is significantly upregulated; however, there are limitations. Competition of electrons from alternative pathways, hydrogenase sensitivity, and inefficient light conversion have resulted in the improvement of strains through mutagenesis or targeted genetic engineering. Continued research holds promise to optimize the *C. reinhardtii* strain and growth conditions to make biohydrogen a competitive fuel.

In addition to biohydrogen production, algae lipid metabolism has been extensively studied in *C. reinhardtii*. Research with *C. reinhardtii* focuses on the synthesis of TAGs as a first-generation biodiesel. Once considered a "non-oleaginous" alga, research has shown that when *Chlamydomonas* cells are deprived of nutrients they accumulate considerable amounts of TAGs, especially in strains blocked in starch accumulation (Merchant et al., 2012; Cakmak et al., 2015; Tran et al., 2019). Because of the extensive TAG accumulation, *C. reinhardtii* has been an excellent model to establish algal genes involved in TAG metabolism. In brief, targeted overexpression of TAG metabolic genes (diacylglycerol acyltransferases, DGATs; acyl-ACP esterases, AAE) have been targeted to increase lipid content under nutrient deprived conditions (Blatti et al., 2011; La Russa et al., 2012; Scranton et al., 2015). It is evident that a better understanding of lipid metabolism is required for each strain of *C. reinhardtii* used to fully utilize the algae's potential as a source of TAGs for biodiesel production.

Nutrient deprivation in C. reinhardtii. When exposed to changes in environmental conditions such as temperature and light intensity or to changes in nutrient media, microalgae have been shown to enhance their lipid accumulation (Cakmak et al., 2012; Dean et al., 2010). With nitrogen starvation, differentiation of cells into gametes, accumulation of starch, a degradation of chloroplast membranes, and a decrease in CO_2 fixation rates are observed (Goodenough et al., 2007; Salas-Montantes et al., 2018). Koo et al. (2017) established that under nitrogen deprivation, *C. reinhardtii* mutants yielded twice as much starch than that of the wild type. In this study, starch over-accumulation was studied with a comparative transcriptome analysis where an induction of phosphoglucomutase 1 (PGM1) expression was identified in the mutants (Koo et al., 2017). PGM1 catalyzes the conversion of glucose-1-phosphate and glucose 6-phosphate for the starch biosynthesis pathway. Thus, under nitrogen deprivation, the starch biosynthesis pathway is significantly upregulated. During acclimation to nitrogen deprivation, it has also been reported that *C. reinhardtii* cells accumulate significant quantities of starch and form lipid bodies (Ball et al., 2009; Chochois et al., 2009; Koo et al., 2017).

On the other hand, sulfur is an essential component present in proteins, lipids, and carbohydrates. In microalgae, sulfur anion is essential for the association of metal ions to proteins and is a component in metabolites that participates in photo-protection (Salas-Montantes et al., 2018). To adapt to sulfur deprivation, *C. reinhardtii* will inactivate photosystem activity, consume dissolved oxygen under light and increase H_2 production (Grechanik et al., 2020). At a certain point, the catabolism of starch begins to contribute electrons to H_2 production to enhance the survivability (Tsygankov & Abdullatypov, 2016).

A study conducted by Cakmak et al. compared the effects that nitrogen deprivation elicited on the wild-type strain of C. reinhardtii against the effects that sulfur deprivation had (2012). This study indicated an observed increase in lipid accumulation in *C. reinhardtii* during nitrogen (N) starvation and an increase in anaerobic H_2 production under sulfur (S) deprivation (Dean et al., 2010; Cakmak et al., 2012). Cakmak et al. (2012) established an inverse relationship between protein concentration in algal samples in response to nitrogen and sulfur starvation and to total neutral lipid and starch levels. In the study conducted by Cakmak et al. (2012), maximum increase in total lipid content was reported to occur after 4 days of both

nutrient deprivation conditions in the wild-type strain. Although nitrogen and sulfur deprivation have been investigated independently, it is yet to be determined what the combinatory effects of nitrogen and sulfur deprivation would have on lipid accumulation in *C. reinhardtii*.

To assess how nutrient deprivation affects *C. reinhardtii*, a chlorophyll content analysis is typically done to establish growth conditions in the cells. To assess the growth of the *C. reinhardtii* cells, Zhang et al. (2020) established that under different cultivation conditions the utilization of cell density and chlorophyll content analyses were essential in establishing the growth of the microalgae under different growth conditions. Transcriptional expression analyses are also utilized to assess the expression levels of genes in the lipid biosynthesis pathway. In a study conducted by Atikij et al. (2019), a RT-PCR analysis revealed that genes involved in fatty acid biosynthesis, such as Acetyl-CoA carboxylase (ACCase) and pyruvate dehydrogenase E1 component (PDH2), were upregulated under salinity deprivation.

The sta6 mutant, cc5373. C. reinhardtii starch mutants have been isolated from wild-type strains. The *sta6* mutant is one of the mutant strains isolated, it exhibits a single-gene disruption that results in a starchless phenotype (Ball, 1998; Ball, 2002; Ball & Deschamps, 2009). The *sta6* mutant includes a distinct disruption in the loci responsible for the expression of the small, catalytic subunit of ADP-glucose pyrophosphorylase (AGPase-SS), a regulatory enzyme involved in starch biosynthesis (Ball, 1998). By blocking the starch synthesis pathway, it creates the potential for diverting metabolic precursors into the lipid biosynthetic pathways. In a study by Work et al. (2010), lipids were extracted, derivatized, and quantified from the wild-type strain and the *sta6* strain under conditions of nitrogen deprivation. By GC-FID quantification and laser scanning confocal microscopy, it was determined that the starchless mutant contained approximately 2- to 4- fold more lipids per cell than the wild-type strain, cc124 (Work et al., 2010). The use of a *C. reinhardtii* starchless mutant will allow the investigation in lipid accumulation under a condition of nitrogen and sulfur deprivation.

Changes in gene expression following nutrient deprivation in C. reinhardtii. Many proteins and genes involved in the eukaryotic lipid metabolism are encoded in the *C. reinhardtii* genome. Expressional

levels of these genes in nitrogen deprivation have been extensively studied in the wild-type strain. However, the expression of these genes in the variants of *C. reinhardtii* are poorly understood, and there is a need to characterize their expression under nutrient deprivation. The *Chlamydomonas* genome contains six specific genes encoding for diacylglycerol acyl transferases (DGATs), which are responsible for the last step of TAG biosynthesis. When exposed to nitrogen deprivation, studies have indicated a substantial up-regulation on the expressional level of DGAT genes after 6 days of treatment (Msanne et al., 2012; Xu et al., 2018). Thus, DGAT enzymes are likely to play a role during the period of maximal TAG accumulation under nitrogen deprived conditions (Msanne et al., 2012).

Recent research has facilitated the overexpression of certain enzymes responsible for lipid biosynthesis. Specifically, studies have attempted to overexpress acetyl-CoA carboxylase (ACCase), the first committed and rate-limiting step of fatty acid biosynthesis. This goal is to observe the effects it has on oil accumulation (Hasan et al., 2018; Chen et al., 2019). Overexpression of ACCase in the wild-type strain was reported to increase lipid content by 21.6% after eight days of nitrogen deprivation (Chen et al., 2019). Recent research has also focused on movement of specific substrates towards the lipid biosynthesis. By applying genetic engineering technologies, phosphoenolpyruvate carboxylase (PEPC), have been successfully inhibited to allow its four-carbon substrate to be utilized in the formation of lipid synthesis (Kao and Ng, 2017). PEPC proteins are responsible for the carbon flux that enters the TCA cycle. This enzyme is responsible for the carbon partitioning of substrates that are in competition with lipid synthesis. Thus, by inhibiting and altering the expression of PEPC, researchers have been able to increase the lipid accumulation rate. Studies of the gene expression levels in *C. reinhardtii* under nutrient deprivation can help further understand the potential of microalgae for commercialized biofuel production.

2 MATERIALS AND METHODS

2.1 Strains, cell culturing and harvesting

The cc5373-sta6 strain of *C. reinhardtii* mt^- progeny of the original BAFJ5 sta6 starchless mutant crossed into a 21gr background was obtained from the *Chlamydomonas* Resource Center. Cells were maintained in Tris-acetate-phosphate (TAP) media agar plates at 25℃ under low-intensity light where re-streaking occurred every two weeks. A wire loopful of cells grown from a single colony were grown in 50 mL TAP and served as the starter culture for treatment flasks. Cells were grown in TAP medium under constant light (room light, fluorescent lights) in sterilized flasks and on a rotary shaker at 120 rpm to ensure uniform illumination and to prevent cell settling. Cells were grown to log phase, OD_{750}=0.3-1.2 (Shi et al., 2017; Charoonnart et al., 2019). A calibration curve was also constructed by measuring the absorbance values at OD_{750} over the course of six days to obtain the specific absorbance, 0.8 to use for log phase. An absorbance at 750 nm was used because pigments are out of the 750 nm absorbance range thus 750 nm is treated as a pure light scattering measurement (Griffiths et al., 2011; Chioccioli et al., 2014).

Once the cells reached OD_{750} =0.8, the cells were harvested via centrifugation at 5,000 rpm for 5 min. The supernatant was removed, and pelleted cells were washed thrice with their respective media (TAP-N media to remove nitrogen, TAP-S media to remove sulfur and TAP-NS media to remove nitrogen and sulfur) (Xu et al., 2018). In each washing step the pelleted cells were resuspended in 50% of their original volume using the respective media and centrifuged at 5,000 rpm for 5 min to harvest the cells. After all the washing steps, the pellet was resuspended in 100 mL of its respective media and 25 mL of cells were transferred into 250 mL sterilized flasks and placed on a rotary shaker as depicted in Figure 1. Cells were collected from these flasks for growth and pigment analysis, lipid body analysis and gene expression analysis. All analyses were conducted in duplicates for each of three blocks.

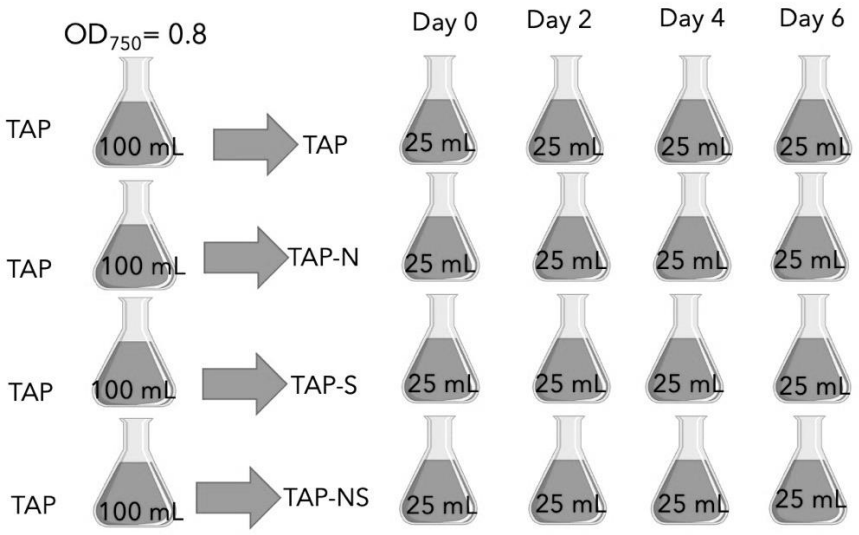

Figure 1. Schematic of experimental design. Cultures for each block were grown in 1000 mL flasks with 100 mL of TAP media until they reached mid-log phase (OD_{750}=0.8). Cells were resuspended in 75 mL of their respective media in a 250 mL and harvested at 120 rpm on a rotary shaker.

2.2 Cell growth measurement

Cell density measurement. Cell density measurement was used to determine and compare cell growth among treatments. Two 1 mL samples were collected from each flask and transferred into a cuvette. The cuvette was placed in a spectrophotometer (Bausch and Lomb, Model Spectronic 20) and absorbance values were measured at OD_{750} (Griffiths et al., 2011; Chioccioli et al., 2014). Sterile TAP, TAP-N, TAP-S, or TAP-NS media was used to blank and calibrate the spectrophotometer for each treatment. Cell density measurements were recorded every 48 hr across a six-day period.

Biomass determination. Fifty mL of cells were taken for day 0 of biomass collection where they were centrifuged at 4,200 rpm for 10 min with supernatant discarded. The pelleted cells were resuspended in 6 mL of Millipore water and centrifuged. The supernatant was discarded. Pelleted cells were resuspended in 5 mL of Millipore water and transferred to empty pre-weighed 15 mL tubes. The pre-weighed tubes with cells were centrifuged and the supernatant removed. The pre-weighted tubes containing the algal biomass were dried in an 80°C oven for 48 hr and weighed. This protocol was repeated at day 4 of starvation (Xu et

al., 2018). Prior to the biomass sampling, twelve empty 15 mL centrifuge tubes were pre-weighed and placed in an oven at 80°C and weighed after 48 hr to measure the average difference in the weight of tubes. The average difference in weight was added to the dry mass obtained from every tube.

2.3 Chlorophyll content determination

Two 3 mL samples were collected from each flask and transferred into sterile 15 mL conical centrifuge tubes. Samples were centrifuged at 4,100 rpm for 10 min and the supernatant removed. The pelleted cells were resuspended in 3 mL of 80% acetone (v/v) and mixed vigorously until the pellet completely dissolved to allow for extraction of chlorophyll from cells. Each tube was placed on a vortex machine at the max setting for 30 sec. The cells were centrifuged once more at 4,100 rpm for 10 min. If the pellet was still green, it would be mixed and centrifuged until the pellet turned white. When the pellet appeared white, 1 mL of the chlorophyll-containing supernatant was transferred into a cuvette for measurement using the spectrophotometer. Absorbance was measured at OD_{750} and $OD_{663.6}$ for chlorophyll A content, and $OD_{646.6}$ for chlorophyll B content. A cuvette containing 80% acetone (v/v) was used as a blank. Samples were collected every 48 hr across a six-day period. Chlorophyll content was calculated utilizing the formulas (Porra et al., 1989):

$$\text{Chlorophyll A } (\mu g/mL) = 12.25\ (A_{663.6}) - 2.55\ (A_{646.6})$$
$$\text{Chlorophyll B } (\mu g/mL) = 20.31\ (A_{646.6}) - 4.91\ (A_{663.6})$$
$$\text{Total Chlorophyll } (\mu g/mL) = 17.76\ (A_{646.6}) + 8.02\ (A_{663.6})$$

2.4 Protein content determination

The protein content of *C. reinhardtii* was measured using the BCA method by Hu et al., 2008 and modified by Xu et al., 2018. Algal cells were harvested and centrifuged at 7,500 g for 10 min. The supernatant was discarded. One mL of 15 mM KH_2PO_4 (pH 4.5) and 2 mL of 20% NaOH were added to the tube and shaken for 30 s. The tube was placed in boiling water for 10 min followed by centrifugation at 7,500 g for 10 min. The supernatant was collected and used to assay the protein content using Pierce BCA protein assay kit (Thermo). Bovine serum was used as the standard sample to obtain the standard curve. Protein content was

calculated from the absorbance measured using the Tecan Microplate Reader at 560 nm and the standard curve.

2.5 Confocal imaging of cells

Qualitative analysis. Two 3 mL samples of the cell culture were placed in a 15 mL centrifuge tube, centrifuged at 2000 g for 5 min, and the supernatant removed. One µL Nile Red (Sigma-Aldrich, Cat. #72485) stock solution containing 1 mg/mL acetone was added and incubated for 5 min at room temperature (Rengel et al., 2018). An eight µL aliquot was placed on a clean glass slide and covered with a coverslip and placed in an incubator at 37℃ for 10 min. The samples were observed with a Nikon ECLIPISE Ti2 Series confocal microscope using a laser excitation line at 488 nm and an emission collected between 620 and 700 nm (Rengel et al., 2018). Chlorophyll fluorescence was captured with a laser excitation line at 633 nm and an emission collected between 620 and 700 nm. The images were merged, and pseudo colored though the NIS-Elements software (Wang et al., 2009). Scans of the algal cells were taken with a 60x oil immersion objective at a pixel resolution of 1024 x 1024 in an 8-bit format (pixel intensity range 0-255). Laser transmission and scan settings remained constant in all scans (Devadasu et al., 2019).

Quantitative analysis. A quantitative analysis was conducted whereby the number of algal cells with and without lipid bodies were counted along with the total number of lipid bodies present per ten fields-of-view (Work et al., 2010; Xu & Pan, 2020). An average lipid body per cell was determined for every 1024x1024 8-bit frame. The average size of lipid bodies per frame was also measured by Nikon NIS-Elements confocal software per field-of-view to compare the treated algal cells versus the control (Raman et al., 2013; Xu & Pan, 2020). The Nikon NIS-Elements confocal software counted and summed all the pixels in the chosen fields that were above the selected threshold of brightness, thereby computing the total area of the above-threshold entities (Wang et al., 2009). The threshold was adjusted by highlighting lipid bodies; if they varied in brightness, the least bright lipid body in the selected field served as the threshold baseline (Wang et al., 2009). The output of each calculation yielded the average lipid body area per frame. It should be noted that

measurements of area underestimate spherical volume and hence yield, but a comparison of areas allows accurate assessment of relative yields from different samples (Wang et al., 2009).

2.6 Genetic expression analysis

RNA extraction. One hundred mL of cells were collected from samples on days 0, 2, 4, and 6 in the TAP, TAP-N, TAP-S, and TAP-NS. RNA was extracted utilizing TRIzol Reagent (Invitrogen) following the instruction provided by the manufacturer. The concentration and purity of the extracted RNA was measured using a Tecan Microplate Reader.

cDNA synthesis and RT-PCR. Single stranded cDNA was synthesized from 2 µg of DNA-digested total RNA following the reverse transcription protocol provided by the manufacturer (Superscript™ III First-Strand Synthesis System). Transcriptional levels of Acetyl-CoA carboxylase (ACCase), phosphoenolpyruvate carboxylase (PEPC), and actin were detected using real-time quantitative PCR. Primers for quantitative real-time RT-PCR were used designed by Xu et al. (2018) shown in Table 1. Real-time quantitative PCR was performed using the iTaq Universal SYBR Green Super Mix (Cat. 1725150, BioRad) following instructions by the manufacturer. The actin gene from *C. reinhardtii* was used as an internal control to normalize the differences between the loading amounts of the template. Each PCR reaction contained 1 µL (8 ng) of cDNA, 10 µ µL of SYBR Green 2x Master Mix, and 1 µL of each gene-specific primer pair (10 mM) to a final volume of 20 µL. PCR was performed as follows: 95˚ C for 10 min followed by 40 cycles at 95˚C for 10s, 60˚C for 1 min, and 72˚C for 30 s. PCR products were analyzed using the Dissociation Curves Software of the CVX96 Touch Real-Time PCR Detection System (Bio-Rad). The $2^{-\Delta\Delta Ct}$ method was used to calculate fold changes of the expressed genes.

Table 1. Primers used for real-time quantitative PCR of lipid biosynthesis enzymes

Gene Name	Primer
ACTIN	F'- ATG GGC CAG AAG GAC TCG TA
	B'- GTC GTC CCA GTT GGT CAC AA
ACCase	F'- CAA GAC TCT GGT TAG CGA TGC
	B'- CCC AAA GCG AGA CAG GAT AG
PEPC	F- CGT GAA CCC CCG TAG AAA AG
	B- CGG AGA CAG TCG TCA AGC AG

2.7 Statistical analysis

For growth, chlorophyll, protein and lipid analyses, an analysis of variance associated with a 4x4 factorial experiment of randomized complete block design was performed. The factorial arrangement was the result of the four levels of treatment (TAP, TAP-N, TAP-S, or TAP-NS) and four levels of time (Day 0, Day 2, Day 4, Day 6). For the genetic analysis, an analysis of variance associated with a 4x2 factorial experiment of randomized complete block design was performed. The factorial arrangement was the result of the four levels of treatment (TAP, TAP-N, TAP-S, TAP-NS) and two levels of time (8 hr and 24 hr). A blocking design was implemented for all experiments in this study, such that it would reduce the variability within blocks from external factors and produce a better estimate of treatment effects. To compare the significant main and interaction effects for all experiments in this study, a post-hoc test in the form of a Tukey's Test and a Bonferroni correction was performed using PROC GLM of the SAS 9.4 statistical and SPSS 27 software. Mean results of all studies were generated from three replications and expressed as mean $\pm$SD. The usual levels of type-1 error rates were used (i.e., * if $p<.05$, ** if $p<.01$ and *** if $p<.001$).

3 RESULTS AND DISCUSSION

3.1 Cell growth, chlorophyll and protein analysis

Cell growth. To determine the growth characteristics of cc5373-sta6, cell density measurements as well as biomass determinations were conducted. The results of cell density measurements showed that the treatments ($F_{(3,6)}$=34.5, p<.001), days ($F_{(3,9)}$=172.03, p<.001) and interactions of treatment and day ($F_{(9,24)}$=15.23, pM<.001) were significantly different among each other (Figure 2, Table 2). Given that there is significant interaction, the emphasis is on the nature of this interaction which is depicted in Figure 2. In the control (TAP), TAP-N, and TAP-S, cc5373-sta6's cell density increased after two days, reached a plateau after four days, and decreased after six days (Figure 2). Interestingly, the interaction between cc5373-sta6 cells subjected to TAP-NS over the course of six days displayed a gradual increase in cell density ($F_{(9,24)}$=15.23, p<.001). (Figure 2). No conclusion nor assumption can be made yet as to what accounts for the increasing trend in cell density in TAP-NS cell. However, nutrient deprivation has been known to cause lipid over accumulation in *C. reinhardtii* cells and could account for the increasing trend in cell density observed in TAP-NS (Sung et al., 2019; Zhu et al., 2021 Potijun et al., 2021).

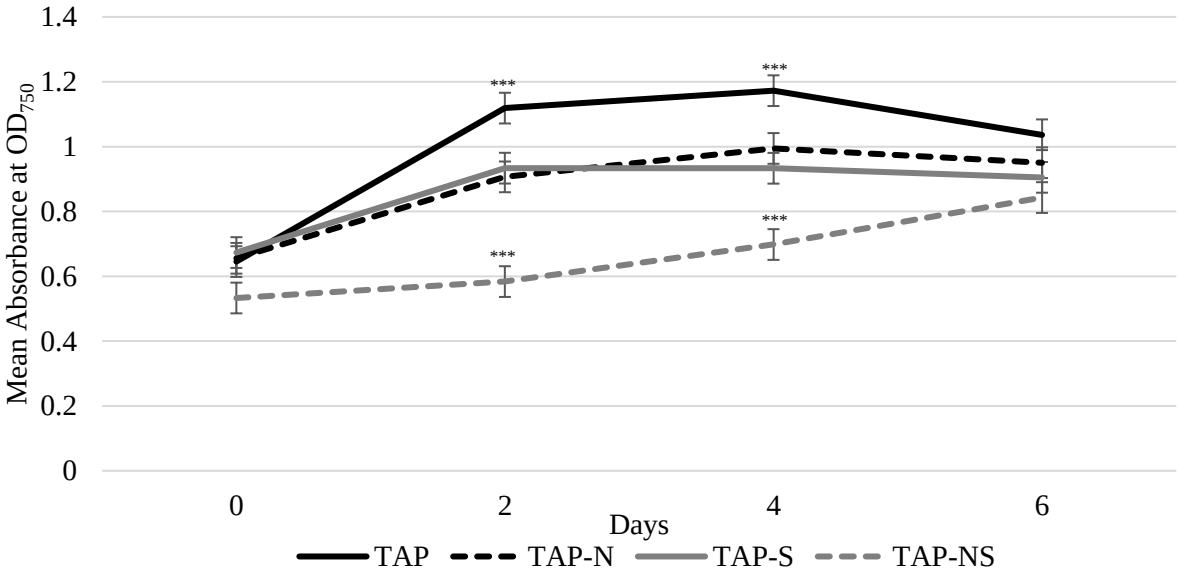

Figure 2. Cell density of strain cc5373-sta6. Samples were obtained every 48 hr for six days after nutrient starvation treatments (TAP, TAP-N, TAP-S, TAP-NS). Means were determined from three replicates. Bars within treatment, non-overlapping 95% confidence intervals indicate significant difference $\alpha = .01$.

Table 2. Analysis of Variance for Cell Density

Source	DF	Type III SS	Mean Square	F Value	Pr > F
Blk	2	0.00126095	0.00063047	0.1	0.9087
Trmt	3	0.66974669	0.2232489	34.46	0.0004
Blk*trmt	6	0.03887272	0.00647879	4.1	0.0057
Day	3	0.81624594	0.27204865	172.03	<.0001
Trmt*day	9	0.21678619	0.02408735	15.23	<.0001
Error	24	0.03795300	0.00158138		

R^2= 0.978687 Coefficient of Variation= 4.684498

Cells subjected to nutrient deprivation will lead to a slower growth rate and eventually growth arrest or death of cells (Kamalanathan et al., 2016). During nitrogen limitation, cells will continue to photosynthesize for it allows the rearrangement of intracellular macromolecular pools leading to mobilization of the carbon from proteins to neutral lipid synthesis (Kamalanathan et al., 2016). Cells subjected to sulfur deprivation exhibited a less severe response when compared to the nitrogen deprived cells. Sulfur deprivation leads to a less severe response. This response corresponds to cellular recycling by autophagy and better accumulation of stress marker molecules (carotenoids, TAG, etc.) (Cakmak et al., 2012). In a recent study conducted by Tran et al., it was found that the sta6 mutant exhibited significantly higher levels of lipid peroxidation as compared to controls under nitrogen deprivation (2019). The results of this study suggested that algal cells with impaired starch metabolism cope differently with oxidative stress than the wild type. The increased cellular reactive oxygen species (ROS) could play a dual role in signaling lipid biosynthesis and inducing autophagy of specific cellular components to recycle and fuel lipid production (Tran et al., 2019). Thus, the increase of ROS caused by the deprivation of both nitrogen and sulfur along with the cells ability to accumulate stress markers more rapidly could cause a faster induction of lipid production to allow cells to aggressively maintain their survivability.

Although algal biodiesel production requires a high amount of lipid bodies, the remaining algal biomass is of benefit to the generation of certain other biofuels. The biomass was determined by weighing the dry weight of *C. reinhardtii* cells after four days of treatment. Based on the analysis of variance results, the difference of dry biomass among treatments were not significantly different; however, the dry biomass was significantly different between days ($F_{(3,9)}$=14.14p<0.005) (Figure 3, Table 3).

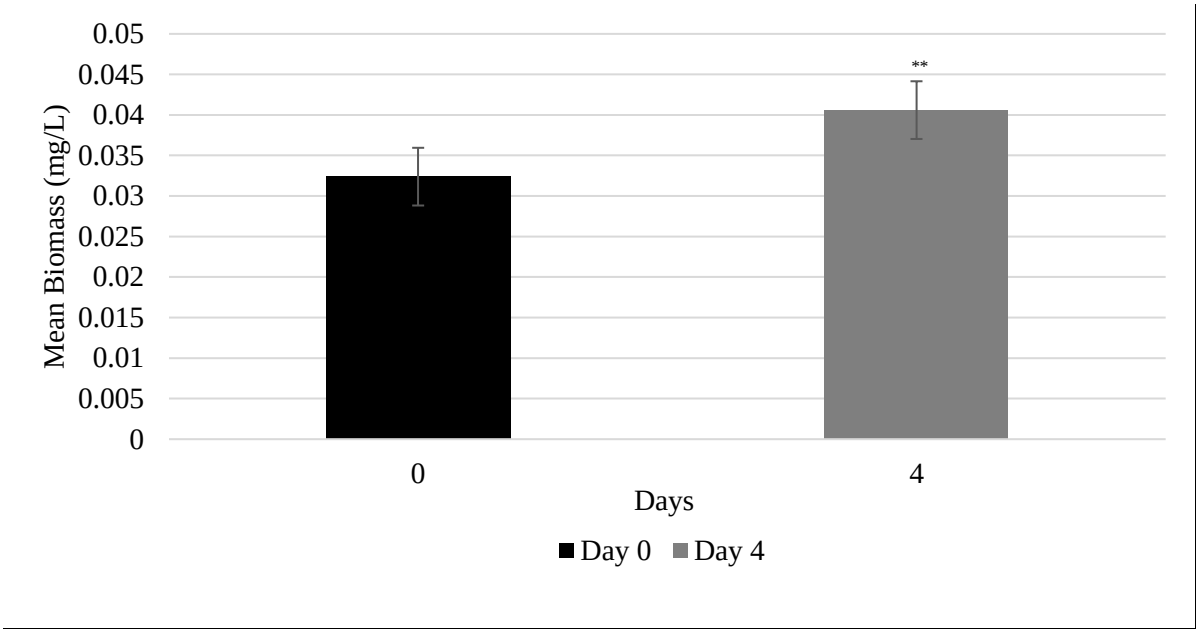

Figure 3. Biomass determination of strain cc5373-sta6. Samples were obtained on Day 0 and Day 4 after nutrient starvation treatments (TAP, TAP-N, TAP-S, TAP-NS). Results were pooled by days for there was no significant difference among treatments. Means were determined from three replicates. Bars within treatment, non-overlapping 95% confidence intervals indicate significant difference α= .01.

Table 3. Analysis of variance for biomass determination.

Source	DF	Type III SS	Mean Square	F Value	Pr > F
Blk	2	0.00050465	0.00025232	11.24	0.0094
Trmt	3	0.00029764	0.00009921	4.42	0.0579
Blk*trmt	6	0.00013475	0.00002246	0.79	0.6049
Day	3	0.00040426	0.00040426	14.14	0.0055
Trmt*day	9	0.00020771	0.00006924	2.42	0.1411
Error	8	0.00022873	0.00002859		

R-Square= 0.871337 Coefficient of Variation= 14.65301

To achieve optimal value, harvesting processes should not interfere with the quality of biomass by causing cell rupture or loss of cellular contents. The high efficiency in biomass should enable reuse of the culture media and have no detrimental impact on the environment (Shin, 2018). In this study, cells subjected to all four treatments accumulated an increase of biomass (dry weight) from Day 0 to Day 4. On the other hand, in a study conducted by Salas-Montantes et al. (2018), they determined that mutant cells deprived of sulfur and nitrogen had a decrease of biomass compared to the TAP medium control. The biomass was determined in cells deprived of nitrogen and sulfur and in a different strain which included overexpression of DNA-binding One Finger (Dof11), a transcription factor that has multiple roles in the regulation of plant physiological processes. Although the biomass decreased overtime, the decrease was not significantly different between the sulfur and nitrogen cells (Salas-Montantes et al., 2018). In our study, there was an overall increase among all treatments when comparing Day 0 to Day 4 ($F_{(3,9)}$=14.14, p<.005). This observation can possibly be explained by the use of the starchless mutant in our study. When microalgae suffer environmental stress, their proliferation slows, and they begin to produce energy storage products in the form of neutral lipids or starch. The cc5373-sta6 strain does not produce starch, thus, we can assume that the increase of biomass was a result of algal lipid over accumulation. When cells that reach the mid-log phase are deprived of nutrients, microalgae are reported to accumulate large amounts of neutral lipids for energy storage (Park et al., 2015). An increase in the amount of lipids possibly contributed to the observed increase in biomass in our study. Thus, the cell growth analysis results in this study i.e., biomass productivity and cell density have shown the overall growth and the potential lipid productivity of this microalgal strain under nitrogen and sulfur deprivation.

Chlorophyll a. When subjected to nutrient deprivation, photosynthetic functions are restricted in *C. reinhardtii* cells. Thus, analyzing chlorophyll content by spectrophotometry can be an indicator of *C. reinhardtii* under stress conditions. In this study, nutrient deprivation conditions markedly decreased chlorophyll a concentration (Figure 4). Results showed a significant difference in chlorophyll a content among days ($F_{(3,9)}$=11.84, p<.001). There is also significant difference among treatments ($F_{(3,6)}$= 448.33 ,

p<.001). However, we observed significant interaction effect between treatments and day ($F_{(9,24)}$=29.53, p<0.001). This means that the chlorophyll a content trend across four levels of days varies significantly among treatments. Given that there is significant interaction; the emphasis is on the nature of this interaction which is depicted in Figure 4. At Day 0, the four treatments were not significantly difference from each other. After two days of deprivation, cells subjected to the TAP medium had the highest chlorophyll content and were significantly different from all other treatments. TAP-N and TAP-NS cells decreased in chlorophyll a content; however, were not significantly difference from each other. After four and six days of deprivation, all treatments were significantly different from each other. These results indicate that the combinatory treatments of nitrogen and sulfur starvation restricts the ability of the cells to maintain photosynthetic activities. The restricted photosynthetic function as a result of nutrient deprivation causes algae to alter their metabolic pathways to sustain their survivability.

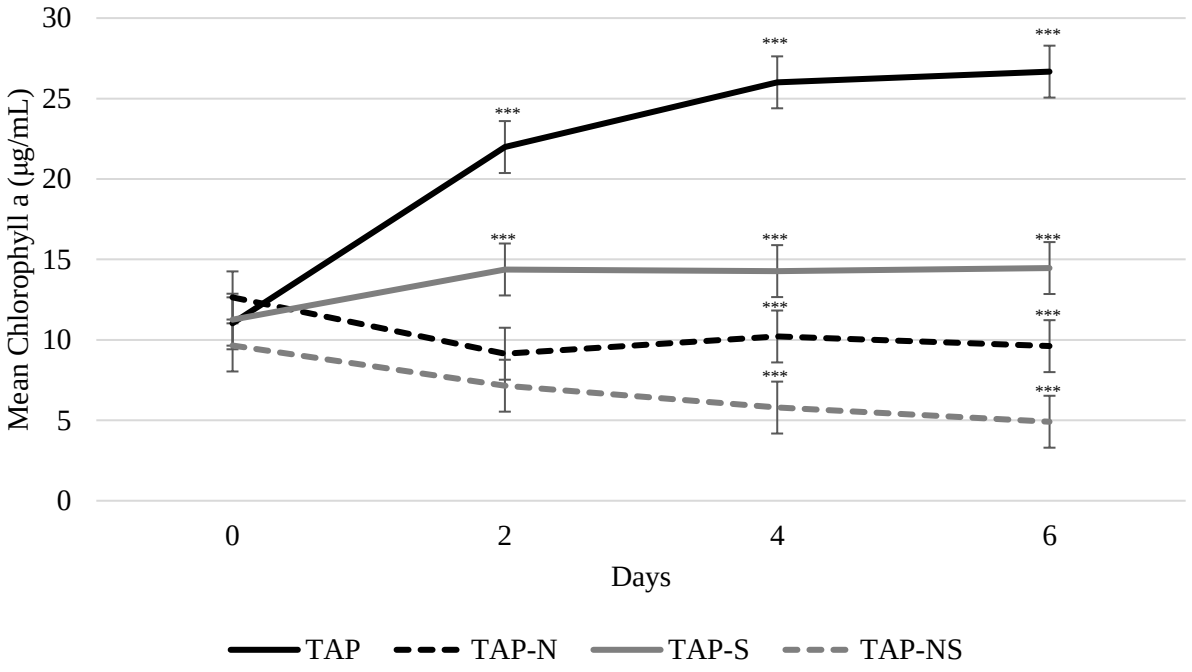

Figure 4. Chlorophyll a content of strain cc5373-sta6. Samples were obtained every 48 hr for six days after nutrient starvation treatments (TAP, TAP-N, TAP-S, TAP-NS). Means were determined from three replicates. Bars within treatment, non-overlapping 95% confidence intervals indicate significant difference α= .01.

Table 4. Analysis of variance for chlorophyll a content

Source	DF	Type III SS	Mean Square	F Value	Pr > F
Blk	2	0.982773	0.491387	0.48	0.6425
Trmt	3	1386.586293	462.195431	448.33	<.0001
Blk*trmt	6	6.185616	1.030936	0.56	0.7562
Day	3	65.201661	21.733887	11.84	<.0001
Trmt*day	9	487.724749	54.191639	29.53	<.0001
Error	24	44.038520	1.834938		

R-Square= 0.977878 Coefficient of Variation = 10.36178

Chlorophyll b. Chlorophyll b content was measured spectrophotometrically every 48 hr under nutrient deprivation. A similar trend was observed in chlorophyll b content as in chlorophyll a (Figure 5, Table 5). We observed significant interaction effect between treatments and day ($F_{(9,24)}$=20.10, $p<0.001$). This means that the chlorophyll b content trend across four levels of days varies significantly among treatments. Given that there is significant interaction; the emphasis is on the nature of this interaction which is depicted in Figure 5. At Day 0, the four treatments were not significantly difference from each other. After two days of deprivation, cells subjected to the TAP medium had the highest chlorophyll content. After two days of deprivation, chlorophyll b content in TAP and TAP-S cells were not significantly different from each other. After two days of deprivation, TAP-N and TAP-NS cell decreased in chlorophyll b content; however, were not significantly difference from each other. After four and six days of deprivation, all treatments were significantly different from each other. These results indicate that the combination of nitrogen and sulfur starvation restricts the ability of the cells to maintain photosynthetic activities. The restricted photosynthetic function as a result of nutrient deprivation cause algae to alter their metabolic pathways to sustain their survivability. Nutrient deprivation restricts the cells' ability to maintain their chlorophyll b content in the same fashion as chlorophyll a.

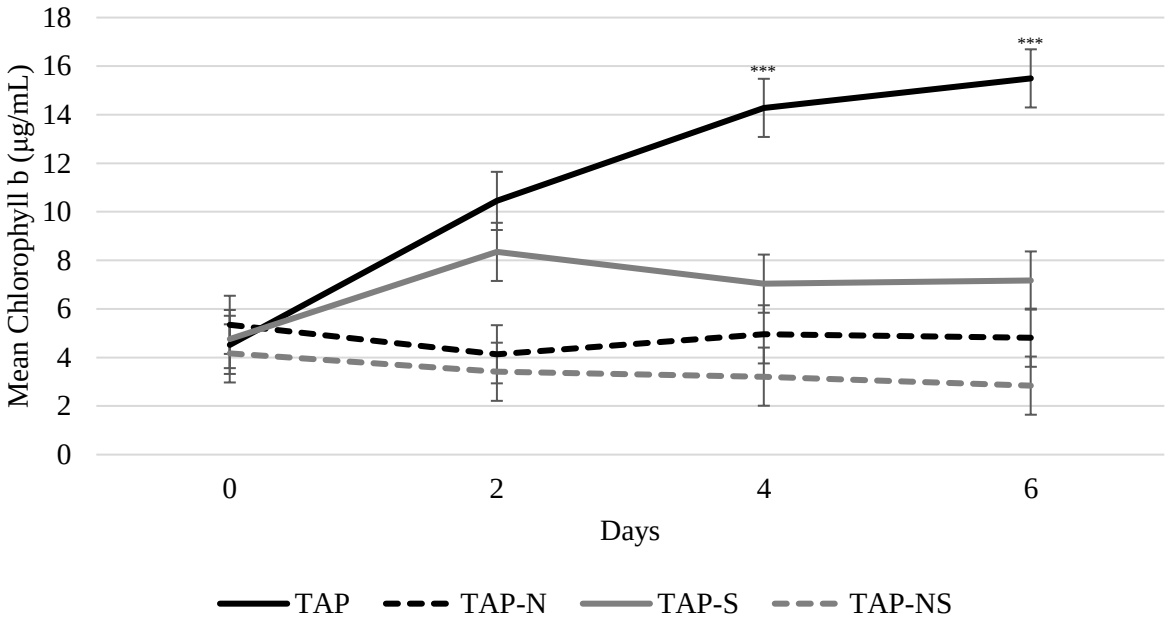

Figure 5. Chlorophyll b content of strain cc5373-sta6. Samples were obtained every 48 hr for six days after nutrient starvation treatments (TAP, TAP-N, TAP-S, TAP-NS). Means were determined from three replicates. Bars within treatment, non-overlapping 95% confidence intervals indicate significant difference $\alpha = .01$.

Table 5. Analysis of variance for chlorophyll b content

Source	DF	Type III SS	Mean Square	F Value	Pr > F
Blk	2	0.3495847	0.1747923	0.6	0.5805
Trmt	3	413.5967352	137.8655784	470.33	<.0001
Blk*trmt	6	1.7587461	0.2931243	0.29	0.9358
Day	3	61.9824592	20.6608197	20.45	<.0001
Trmt*day	9	182.7722353	20.3080261	20.10	<.0001
Error	24	24.2457348	1.0102389		

R-Square= 0.964590 Coefficient of Variation= 15.32398

Total chlorophyll content. Total chlorophyll content was measured spectrophotometrically every 48 hr and calculated by adding $OD_{646.6}$ and $OD_{663.6}$. Results of total chlorophyll content determination exhibited a similar trend as chlorophyll a and b (Figure 6, Table 6). We observed significant interaction effect between treatments and day ($F_{(9,24)}$=26.88, $p<0.001$). This means that the total chlorophyll content trend across four levels of days varies significantly among treatments. Given that there is significant

interaction, the emphasis is on the nature of this interaction which is depicted in Figure 6. At Day 0, the four treatments were not significantly difference from each other. After two days of deprivation, cells subjected to the TAP medium had the highest chlorophyll content and were significantly different from all other treatments. TAP-N and TAP-NS cells decreased chlorophyll b content; however, were not significantly difference from each other after two days. After four and six days of deprivation, all treatments were significantly different from each other. These results indicate that the combination of nitrogen and sulfur starvation restricts the ability of the cells to maintain photosynthetic activities. The restricted photosynthetic function as a result of nutrient deprivation cause algae to alter their metabolic pathways to sustain their survivability.

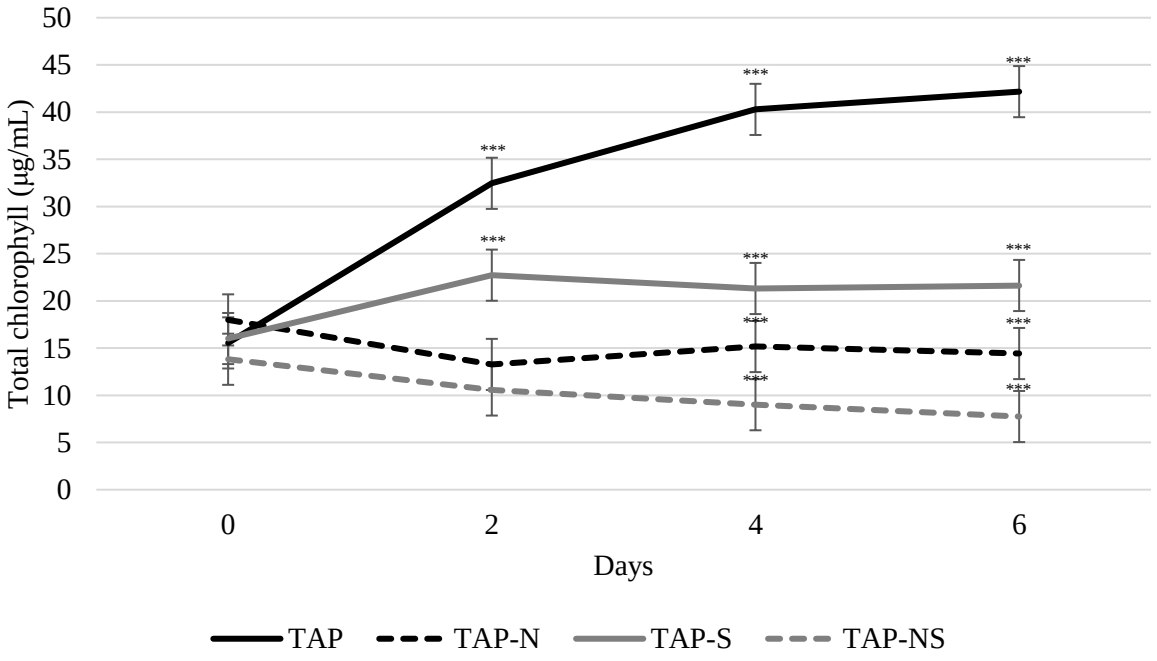

Figure 6. Total chlorophyll content of strain cc5373-sta6. Samples were obtained every 48 hr for six days after nutrient starvation treatments (TAP, TAP-N, TAP-S, TAP-NS). Means were determined from three replicates. Bars within treatment, non-overlapping 95% confidence intervals indicate significant difference $\alpha = .01$.

Table 6. Analysis of variance for total chlorophyll Content.

Source	DF	Type III SS	Mean Square	F Value	Pr > F
Blk	2	2.428489	1.214245	0.51	0.6244
Trmt	3	3313.535848	1104.511949	463.89	<.0001
Blk*trmt	6	14.285945	2.380991	0.46	0.8302
Day	3	253.482541	84.494180	16.35	<.0001
Trmt*day	9	1249.857303	138.873034	26.88	<.0001
Error	24	124.011528	5.167147		

R-Square= 0.974986 Coefficient of Variation= 11.57779

C. reinhardtii starchless mutant cells subjected to nutrient deprivation displayed a decrease in overall chlorophyll content. Additionally, our results indicated a decrease in chlorophyll a + b content in both treatments of nitrogen deprivation. In a study conducted by Song et al., when nitrogen was deprived in marine microalgae *Dunaliella tertiolecta* there appeared to be an inhibition of cell chlorophyll accumulation after one day of deprivation and a significant inhibition after several days of cultivation (2016). In addition, a study conducted by Cakmak et al. (2012), reported a decrease in chlorophyll content on the *C. reinhardtii* wild type strain, cc124, after one day of deprivation. In recent studies, researchers have been utilizing melatonin to facilitate the coordination of cell growth and lipid accumulation in *C. reinhardtii* under nitrogen stress (Meng et al., 2020). Meng et al. reports that the use of melatonin weakens the nitrogen stress-induced oxidative damage by delaying the chlorophyll loss that is typically observed after 24 hr (2020). Thus, the results by Song et al. (2016), Cakmak et al. (2012), and Meng et al. (2020) support our finding of significant reduced chlorophyll accumulation observed after 48 hr of deprivation, especially in cells deprived of nitrogen. In this study, although chlorophyll a + b content was lower as compared to the TAP control, cells were still able to maintain their low levels after six days of nutrient deprivation.

The changes in chlorophyll content are known to stabilize after four days of deprivation for stress leads to autophagy in order to recycle part of the cytoplasm including the organelles (Cakmak et al., 2012). Because nitrogen is the most important nutrient element contributing to the growth of microalgae cells, its

limitation alters the biosynthesis of cellular pigments, chlorophylls and carotenoids. For example, 5-aminolevulinic acid, precursor for chlorophyll synthesis is synthesized by succinate and glycine or directly from glutamate (Fufsler et al., 1984; Kamalanathan et al., 2016). Nitrogen limitation affects the synthesis of amino acids like glycine and glutamate, limiting the synthesis of 5-aminolevulinic acid decreasing the levels of chlorophyll in cells (Kamalanathan et al., 2016). Cells exposed to nitrogen stress can mobilize molecules of chlorophyll a and other pigments as an internal source of nitrogen decreasing the photosynthetic unit (Perry et al., 1981, Kamalanathan et al., 2016).

Although, we have not done carotenoid analysis in our study, it is interesting to note that, β-carotene levels are known to increase in response to decreased chlorophyll b content in order to compensate the reduced cell division and growth rates and to address the oxidative stress (Song et al. 2016). Park et al. (2015) conducted a systems biology analysis to observe the response of *C. reinhardtii* to nitrogen deprivation. Results from electron microscopy and TAG accumulation experiments indicated that the increase in TAG levels coincided with a reduction of chloroplast membrane amounts after 12 hr of deprivation. Oil body diameter was measured at 0.75 μm at 6 hr and had increased six-fold at 24 hr (Park et al., 2015). These results support our chlorophyll content results and suggest that lipid over accumulation is responsible for the overall increase of cell density and biomass observed in nutrient deprived sta6 cells.

Protein content. Total protein content was determined spectrophotometrically every 48 hr using the bicinchoninic acid (BCA) protein assay. Samples and standards of known concentration (20-2,00 μg/mL) were measured at OD_{562}. Absorbance values of samples were compared to standards to determine total protein content. We observed significant interaction effect between treatments and day ($F_{(9,30)}$=49.622, $p<0.001$). This means that the total protein content trend across four levels of days varied significantly among treatments. Given that there is significant interaction; the emphasis is on the nature of this interaction which is depicted in Figure 7. At Day 0, the four treatments were not significantly difference from each other. After two days of deprivation, cells subjected to the TAP medium had the highest protein content and were significantly different from all other treatments. TAP-N, TAP-S and TAP-NS cells decreased in protein content; however, were not significantly difference from each other after two days. The protein

content in all treatments from day 2 was not significantly different from day 4. After six days of deprivation, TAP cells elicited the highest protein content and were significantly different among all other treatments. Although no significant difference was observed between TAP-N and TAP-NS after six days, they exhibited the lowest protein content. These results indicate that the combinatory treatments of nitrogen and sulfur starvation restricts the ability of the cells to maintain their protein synthesis. The reduced protein content as a result of nutrient deprivation causes algae to alter their metabolic pathways to sustain their survivability.

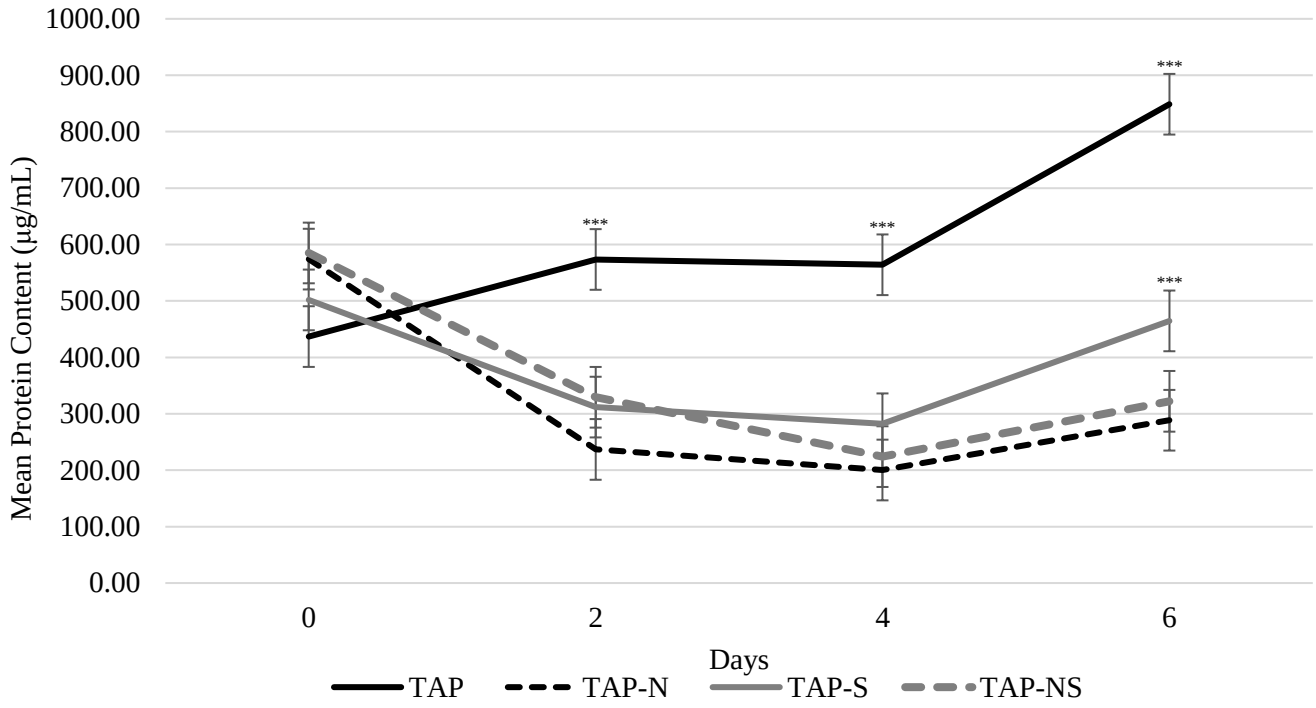

Figure 7. Total protein content of strain cc5373-sta6. Samples were obtained every 48 hr for six days after nutrient starvation treatments (TAP, TAP-N, TAP-S, TAP-NS). Means were determined from three replicates. Bars within treatment, non-overlapping 99% confidence intervals indicate significant difference $\alpha = .01$.

Table 7. Analysis of variance for total protein content.

Source	DF	Type III SS	Mean Square	F Value	Pr > F
Model	18	9953646.05	552980.336	482.049	<.0001
Blk	2	3336.6830	1668.342	1.454	0.250
Trmt	3	569231.06	189743.68	165.405	<.0001
Day	3	340152.38	113384.128	98.840	<.0001
Trmt*day	9	512308.97	56923.218	49.622	<.0001
Error	30	34414.365	1147.145		

R-Square= 0.997 Adjusted R Squared=0.994

Microalgal cells subjected to nitrogen and sulfur deficiency can cause an increase in lipid content and a decrease in protein content as observed in the results of our study. The increase in TAG accumulation after nitrogen deprivation is known to attribute a turnover of nitrogen-rich compounds that provide carbon/energy for TAG synthesis (Cakmak et al., 2012; Schmollinger et al., 2014; Song et al., 2016). In a study conducted by Sierra et al., a kinetic study was performed to evaluate *C. reinhardtii* protein accumulation in TAP-N and TAP conditions (2017). Protein accumulation decreased after 96 hr under nitrogen deprived conditions. Photosynthetic proteins (i.e., RuBisCo proteins, light harvesting complex proteins) are known to be degraded decreasing overall protein content and photosynthetic activity (Sierra et al., 2017). Additionally, in a study conducted by Xu et al., found protein levels to significantly decrease in *C. reinhardtii* subjected to nitrogen deprivation causing the protein to transform into lipid or carbohydrates (2018). Being that the cells subjected to nitrogen and sulfur deprivation decreased in chlorophyll and protein content, we proceeded to analyze the lipid (TAG) accumulation via confocal microscopy analysis.

3.2 Lipid body analysis

Qualitative analysis of lipid bodies. To further characterize the response to nitrogen (N) and sulfur (S) starvation in the starchless mutant cc5373-sta6, total lipid accumulation was observed via confocal microscopy every 48 hr for six days. Nile Red staining allowed for the visualization of lipid accumulation

by staining lipids yellow and chlorophyll content red. Qualitatively, lipid accumulation was observed after 48 hr in all deprivation conditions (Figure 7). TAP-S and TAP-NS cells showed the highest amount of lipid bodies indicated by the increased yellow staining of lipid bodies (Figure 7). After four days of deprivation, accumulation of lipids in TAP-N and TAP-NS were more noticeable as compared to Day 2 (Figure 7). It was observed that after four days of deprivation TAP-S cells increased in size and released free-floating lipids (Figure 7). With TAP (control), there was a low yield of lipid accumulation; however, these cells did increase in number and in size over the course of the six-day period (Figure 7). After six days of nutrient deprivation, TAP-N cells showed the highest amount of lipid bodies, whereas TAP-S and TAP-NS cells sustained their lipid content (Figure 7). The combinatory effects of N and S deprivation may have affected not only photosynthetic and metabolism components of the cell but also lipid synthesis.

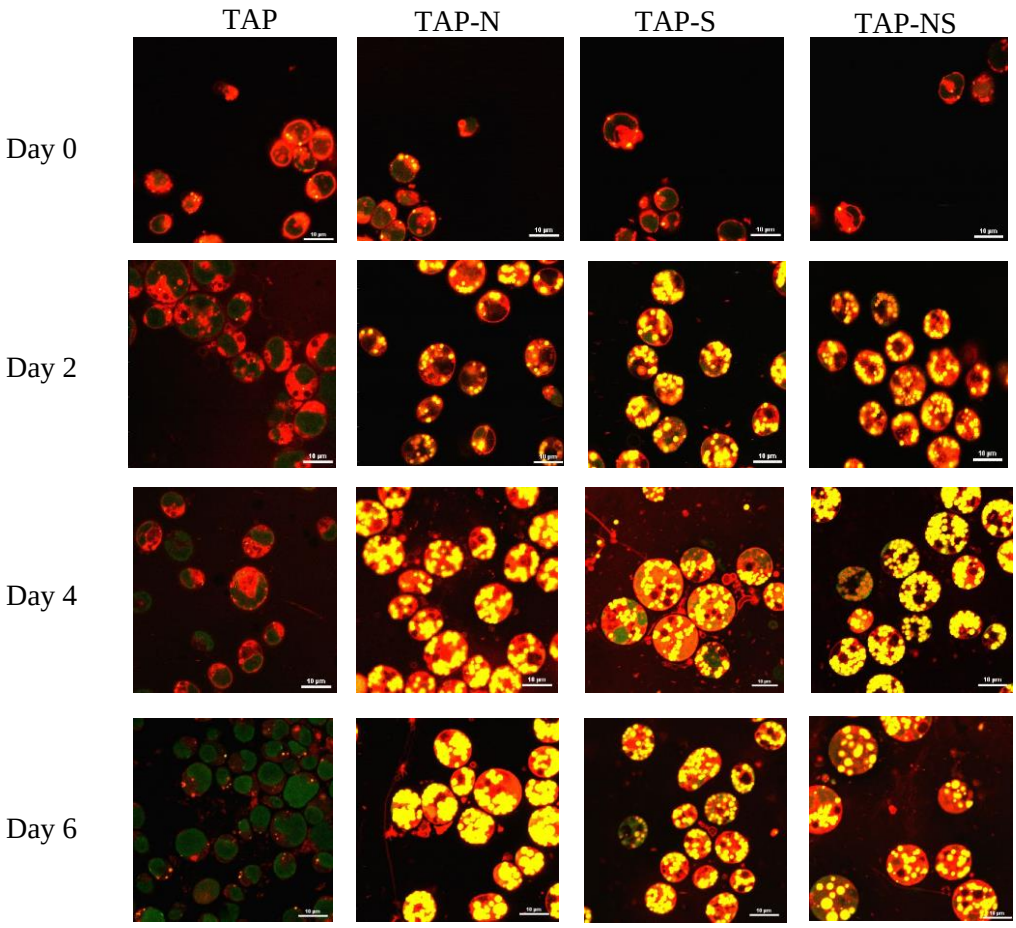

Figure 8. Qualitative confocal analysis of strain cc5373-sta6 under nutrient deprivation. Cells were viewed under the confocal microscope after 48 hr of nutrient deprivation and stained with Nile Red staining to observe lipid accumulation. Representative images were selected from ten fields of view per treatment.

Determination of lipid body number per cell. To analyze the lipid accumulation per cell when exposed to nutrient deprivation, a quantitative analysis was performed. The number of lipid bodies present in each cell was counted. The number of lipid bodies and cells was counted in ten randomized fields of view (1024 x 1024) to obtain an average number of lipid bodies per cell (Figure 8). Our results indicated that there was significant difference for days ($F_{(3,9)}$=5.412, p<.005 and treatment ($F_{(3,6)}$=22.622, p<.001), but there was no significant interaction between days and treatment ($F_{(9,24)}$ =0.936, p=0.520) (Table 7). In this regard, results were pooled by treatments to observe the average lipid body number per cell. Although the lipid body number per cell was not significantly different among the nutrient deprivation conditions, they were still significantly different than the TAP control. These results provide evidence for lipid accumulation to occur as a result of nutrient deprivation. It is interesting to note that the average number of lipid bodies per cell was highest in TAP-S; however, there was a lower count of cells present in these fields of view (Figure 8). Although these cells did have the highest number of lipid bodies per cell, there was no significant difference in lipid body number among the treatments (Figure 8, Table 7). It was observed that S limitation decreased cell proliferation due to the decreased number of cells compared to other treatments. However, this trend was not observed in cells subjected to both N and S deprivation.

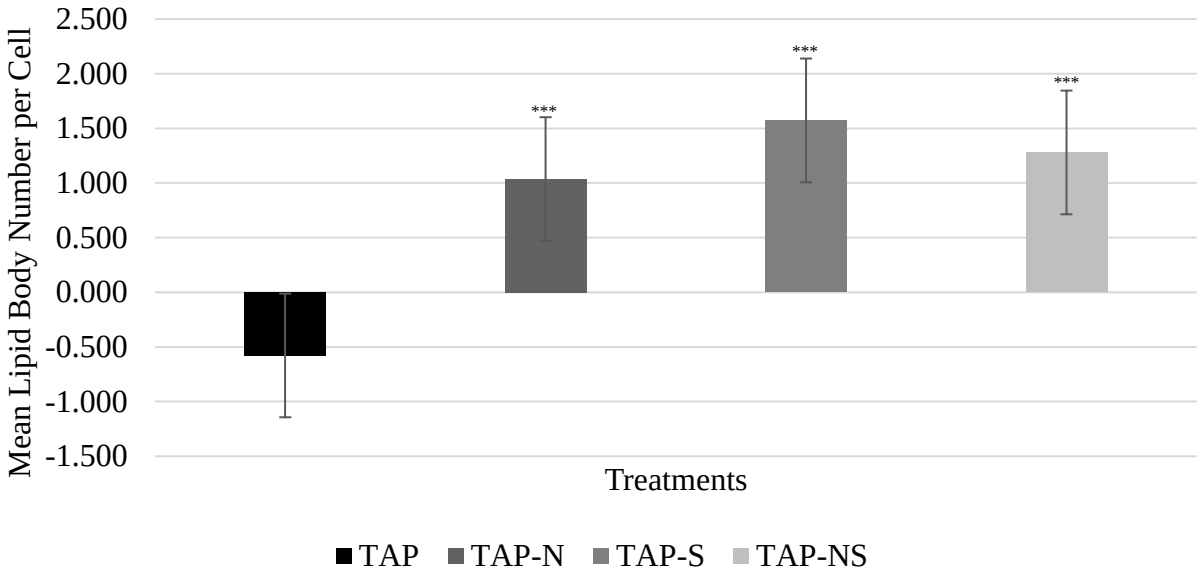

Figure 9. Average lipid bodies per cell of strain cc5373-sta6 under nutrient deprivation. Lipid bodies and cells were counted per frame to obtain an average number of lipid bodies per cell. Means were determined from three replicates. Results were pooled by treatment for there was no significant difference among time intervals. Bars within treatment, non-overlapping 99% confidence intervals indicate significant difference $\alpha = .01$.

Table 8. Analysis of variance for average lipid bodies per cell

Source	DF	Type III SS	Mean Square	F Value	Pr > F
Blk	2	2.395	32.887	2.438	0.109
Trmt	3	33.337	11.112	22.622	<0.001
Blk*trmt	6	0.835	0.139	0.283	0.939
Day	3	7.975	2.658	5.412	0.005
Trmt*day	9	4.095	0.455	0.936	0.520
Error	24	11.789	0.491		

R-Square= 0.805 (Adjusted R-Squared= 0.618)

Measurement of lipid body size. To assess the overall amount of lipid accumulation in the cell, lipid bodies (droplets) were measured using the Nikon NIS-Elements confocal software. The size of lipid bodies was measured every 48 hr for six days across ten fields of view (1024x1024) to obtain an average lipid body size. We observed significant interaction effect between treatments and day ($F_{(9,24)}$=20.783, $p<0.001$). This means that the trend for average lipid body size across four levels of days varies significantly among

treatments. Given that there is significant interaction, the emphasis is on the nature of this interaction which is depicted in Figure 9. On Day 0, there was no significant difference observed among all treatments as observed in the qualitative confocal images (Figure 7). After two days of nutrient deprivation, the average lipid body size among all treatments were significantly different from each other. TAP-NS cells exhibited the largest lipid body size among all treatments. After four days of deprivation, there was no significant different observed among nutrient deprivation, however all deprivation conditions were significantly different from TAP control. After six days of deprivation, TAP-S and TAP-NS cells displayed the highest average lipid body size, however they were not significantly different from each other. Although TAP-N cells displayed a lower lipid body size, they were still significantly different from the TAP control. These results showcase that depriving cells from both N and S allows for lipid overaccumulation to occur and elicits the largest lipid body size after 48 hr.

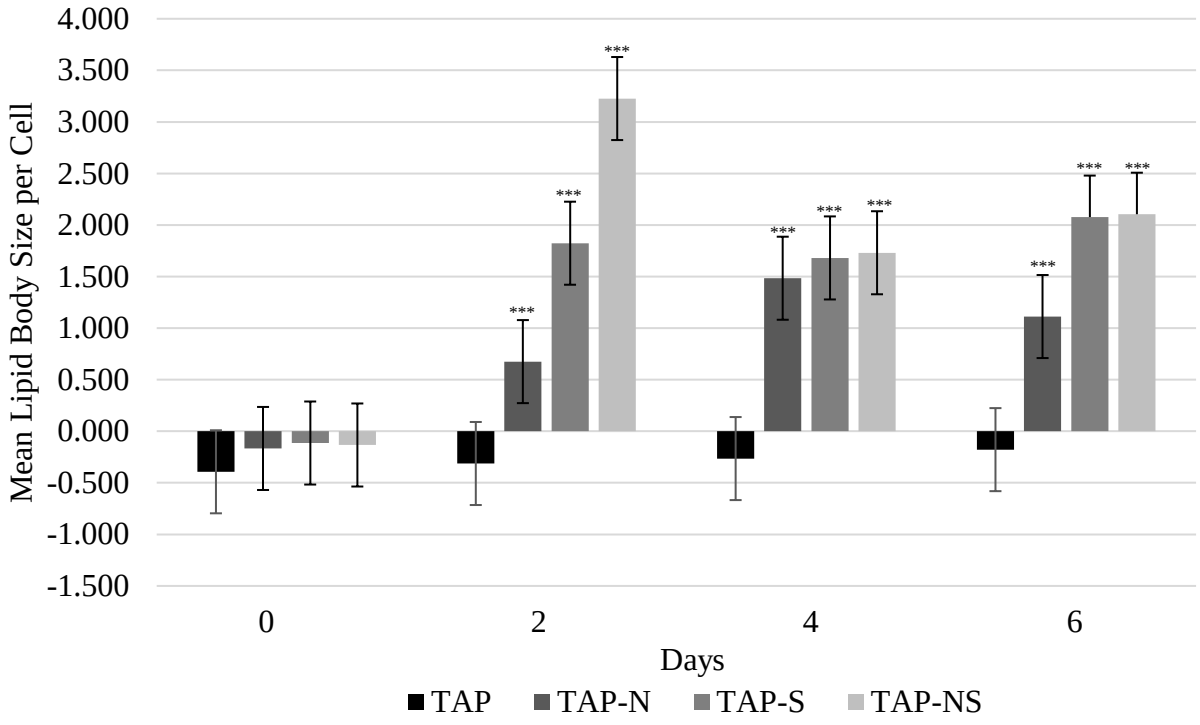

Figure 10. Average size of lipid bodies per treatment of strain cc5373-sta6 under nutrient deprivation. Mean values were determined from three replicates. Bars within treatment, non-overlapping 99% confidence intervals indicate significant difference $\alpha = .01$.

Table 9. Analysis of variance average size of lipid bodies

Source	DF	Type III SS	Mean Square	F Value	Pr > F
Blk	2	0.672	0.336	5.403	0.012
Trmt	3	19.554	6.518	104.836	<0.001
Blk*trmt	6	0.479	0.080	1.285	0.301
Day	3	28.027	9.342	150.264	<0.001
Trmt*day	9	11.629	1.292	20.783	<0.001
Error	24	1.492	0.062		

R-Square= 0.976 (Adjusted R-Squared= 0.953)

Cells subjected to nutrient deprivation accumulate lipids as a result of stress. Our study indicated that overall accumulation of TAG increased significantly in all nutrient deprived conditions compared to the control. Sathe et al. (2019) quantified lipid accumulation by staining cells with Nile red and measuring fluorescence intensity at 580 nm. Cells cultured in 0 μM N had significantly higher fluorescence (indicating higher lipids) than cells cultured in 700 μM N (Sathe et al., 2019). In addition, transmission electron microscopy results demonstrated typical features associated with programed cell death, such as chloroplasts being degraded into smaller sphere-like sub-compartments (Cakmak et al., 2012). Images in the same study also displayed cytoplasmic lipid droplets under N deprivation (Cakmak et al., 2012; Sathe et al., 2019). In our study, the confocal microscope was used to observe lipid bodies after six days of nutrient deprivation. In regard to lipid accumulation, cells in our study displayed increased lipid accumulation that correlates to the results supported by the aforementioned studies.

It has been reported that cell enlargement occurs specifically when cells are deprived of S (Kamalanathan et al., 2016). In addition to an increase of lipid over accumulation of cells, cell enlargement was of interest in our study. Cell enlargement was assessed by the number of lipid bodies found in each cell. Although there was no significant different among all treatments, cells deprived of S exhibited the highest number of lipid bodies present consistent with the increased cell enlargement found in Kamalanathan et al. (2016). In our study, it was observed that cells subjected to S were the largest in size after four days of deprivation. These images also showcased free-floating lipid droplets as a result of cells

bursting (Figure 7). Compared with S-starved cells, N-starved cells displayed a lower amount of lipid bodies per cell and with lower amount of enlargement. This may be correlated with the greater metabolic stress N-starved samples undergo (Park et al., 2015; Schmollinger et al., 2014; Cakmak et al., 2012). It is known that starch and neutral lipids greatly accumulate in nutrient deprived cells and those increases correspond to the rapid decrease in protein levels (Cakmak et al., 2012). However, being that our study utilized a starchless mutant, we can only assume that the cell enlargement may be caused solely by lipid over accumulation.

One way we chose to characterize the content of lipids in our cells was by averaging the lipid body size across all treatments. Cells subjected to both nitrogen (N) and sulfur (S) deprivation displayed the highest lipid body size after 48 hr of deprivation. It was observed that NS deprived cells maintain their lipid body size over the course of 6 day-deprivation. In a study conducted by Sung et al. (2019), lipid content of mutant strains was obtained by density gradient centrifugation. Cells extracted from the upper part (least dense) of the density gradient had a relatively high total fatty acid methyl ester (FAME) content (Sung et al., 2019). The proportion of unsaturated fatty acids having a relatively low density in mutant strains was 71.4%; the ratio of C18/C16 fatty acids was 1.27 (Sung et al., 2019). The ratio of C18/C16 was reported as 1.18 and 1.03 of mid and bottom phases respectively. These results of Sung et al.'s study indicated that the microalgal mutant strains with relatively low cell densities have higher total lipid content, a higher number of carbon chains with lower density, and higher unsaturated fatty acid ratios (Sung et al., 2019).

The results of our study showed cells subjected to TAP-NS after two days these cells displayed a larger size of lipid bodies among all treatments. Based on our findings, it would be an advantage and recommended to cultivate cc5373-sta6 cells under N and S deprivation for two days to increase the proportion of lipids produced. The most common fatty esters contained in biodiesel are palmitic, stearic, oleic, linoleic, and linolenic (Salas-Montantes et al., 2018; Knothe, 2008). It is also reported that fatty acid profiles change with nutrient deprivation (Iwai et al., 2014). Therefore, the determination of the lipids and fatty acid contents e.g. FAME analysis of cc5373-sta6 under nitrogen and sulfur deprivation especially at

two days warrants attention. This is to determine if cc5373-sta6 could meet the required fatty acid composition for biodiesel production.

3.3 Gene expression analysis

RNA isolation. To further establish the effects of nutrient deprivation on lipid accumulation of cc5373-sta6, the expression levels of specific enzymes in lipid accumulation were investigated. RNA isolation was done every 48 hr over six days. The yield of RNA from cells subjected to TAP medium after all 48 hr intervals was substantial to carry on a genetic analysis; however, cells in nutrient deprivations (TAP-N, TAP-S, TAP-NS) had low RNA yields (Table 9). RNA was isolated at 48 h intervals to correspond with our chemical and microscopy analyses. However, as mentioned previously our results were low RNA yields at Day 2, 4 and 6. An analysis of total RNA levels by Park et al. (2015) showed a decrease in RNA after 6 hr of N starvation; this was attributed to the degradation of purines and pyrimidines from RNA breakdown that appears to contribute N for protein synthesis during the first 24 hr of deprivation. The results found by Park et al.'s justifies the low RNA yield obtained with our RNA isolation every 48 hr over six days (2015).

Metabolic pathways of *C. reinhardtii* cells were reported to be altered after 4 hr of nutrient deprivation. Thus, in our experiments, RNA isolation and determination of gene expression levels were done at 8 hr and 24 hr intervals. We aimed to determine the expression levels of ACCase and PEPC at 8 hr and 24 hr. ACCase and PEPC were enzymes reported to be affected by nutrient deprivation and have affected lipid metabolism (Wang et al., 2017; Xu et al., 2018; Chen et al., 2019). RNA isolated from cells after the 8 hr and 24 hr nutrient deprivations gave a much higher yield and with purity between the 1.7-2.0 ratio (Table 10). Purification of RNA from *C. reinhardtii* cells was determined spectrophotometrically at OD_{260} and OD_{280} via the Tecan Microplate Reader. Previous studies that isolated RNA from *C. reinhardtii* have reported a purity range of 1.7-2.0 (Willfinger et al., 1997; Kim et al., 2014; Valledor et al., 2014).

Table 10. Concentration and $OD_{260/280}$ ratio of total RNA isolated from cc5373-sta6 at Day 0, 2, 4 and 6.

Time	Media	OD260	OD280	Conc (ng/uL)	Ratio
Day 0	TAP	0.1305	0.0588	104.4	2.22
	TAP-N	0.1063	0.0455	85.04	2.34
	TAP-S	0.0739	0.0332	59.12	2.23
	TAP-NS	0.0774	0.0391	61.92	1.98
Day 2	TAP	0.121	0.057	96.8	2.12
	TAP-N	0.0046	0.0042	3.68	1.10
	TAP-S	0.0229	0.0043	18.32	5.33
	TAP-NS	0.0025	0.0016	2.00	1.56
Day 4	TAP	0.3132	0.1463	250.56	2.14
	TAP-N	0.0352	0.0186	28.16	1.89
	TAP-S	0.0109	0.0076	8.72	1.43
	TAP-NS	0.0225	0.014	18.00	1.61
Day 6	TAP	0.1771	0.0855	141.68	2.07
	TAP-N	0.0266	0.0129	21.28	2.06
	TAP-S	0.0169	0.0099	13.52	1.71
	TAP-NS	0.0163	0.0087	13.04	1.87

Table 11. Concentration and $OD_{260/280}$ ratio of total RNA isolated from cc5373-sta6 after 8 hr and 24 hr.

Time	Media	OD260	OD280	Conc (ng/uL)	Ratio
8 hr	TAP	0.6625	0.386	662.5	1.72
	TAP-N	0.4609	0.2712	460.9	1.70
	TAP-S	0.8493	0.4996	849.3	1.70
	TAP-NS	0.8706	0.5084	870.6	1.71
24 hr	TAP	0.6866	0.402	686.6	1.71
	TAP-N	0.8715	0.5102	871.5	1.71
	TAP-S	0.8941	0.5191	894.1	1.72
	TAP-NS	0.5953	0.3474	595.3	1.71

To further establish the 8 hr and 24 hr time intervals in our experiments, we turned to a study by Schmollinger et al. (2014). This study identified that the highest mRNA abundance of two-protein sub-units of ACCase were at 4, 8, 12 and 24 hr (Schmollinger et al., 2014). It was found that mRNAs encoding the different ACCase subunits are repressed early upon nitrogen (N) deprivation and then recovered to N-replete levels between 12 to 24 hr (Schmollinger et al., 2014). This study gave us a baseline of time intervals to harvest cells and extract RNA. The 8 hr and 24 hr time frame are beginning stages of the purine and pyrimidine degradation (Park et al., 2015). Therefore, it is likely optimal to isolate RNA no longer than 24 hr, before nucleotides become significantly degraded.

A study conducted by Hang et al. (2020) investigated the lipid productivity of *C. reinhardtii* with combination of NaCl and $CaCl_2$ stresses. In this study, genes involved in lipid metabolism (glycerol-3-phosphate dehydrogenase, GPDH; lysophosphatidic acid acyltransferase, LPAAT; diacylglycerol acyltransferase, DAGAT) were monitored after 24 hr of salt stress and were significantly upregulated (Hang et al., 2020). The aforementioned studies indicate that cultivation time of 24 hr is an established amount of time to affect cells exposed to nutrient deprivation or stress and observe lipid metabolism alterations. These studies also justify our investigation of the expression levels of ACCase and PEPC after 8 and 24 hr of nitrogen and sulfur deprivation.

ACCase expression level. RNA isolates were reverse transcribed into cDNA and used for amplification to assess expression levels of ACCase regarding treatments after 8 hr and 24 hr. The average Ct value for actin was 18.0. After normalizing our genes of interest to our housekeeping gene, we found our ACCase Ct values in our TAP control to exhibit an average of 22.0 and 25.2 respectively. We observed significant interaction effect between treatments and day ($F_{(3,14)}$=3.953, $p<0.05$) (Table 11). This means that the trend for ACCase expression across four levels of days varies significantly among treatments. Given that there is significant interaction, the emphasis is on the nature of this interaction which is depicted in Figure 10. As compared to the TAP control, cells subjected to TAP-N increased in ACCase expression levels after 8 hr (one-fold) and 24 hr (two-fold). Cells subjected to TAP-S decreased in ACCase expression after 8 hr and 24 hr as compared to the control. Cells subjected to TAP-NS displayed the largest increase in ACCase expression. After 8 hr of N and S deprivation (TAP-NS), expression of ACCase increased two-fold as compared to the TAP control. Likewise, after 24 hr deprivation, cells subjected to N and S deprivation had an increased ACCase expression, three-fold increase compared to the TAP control (Figure 10). Thus, the deprivation of both nitrogen and sulfur causes an increase in lipid biosynthesis after 8 hr and 24 hr in cc5373-sta6.

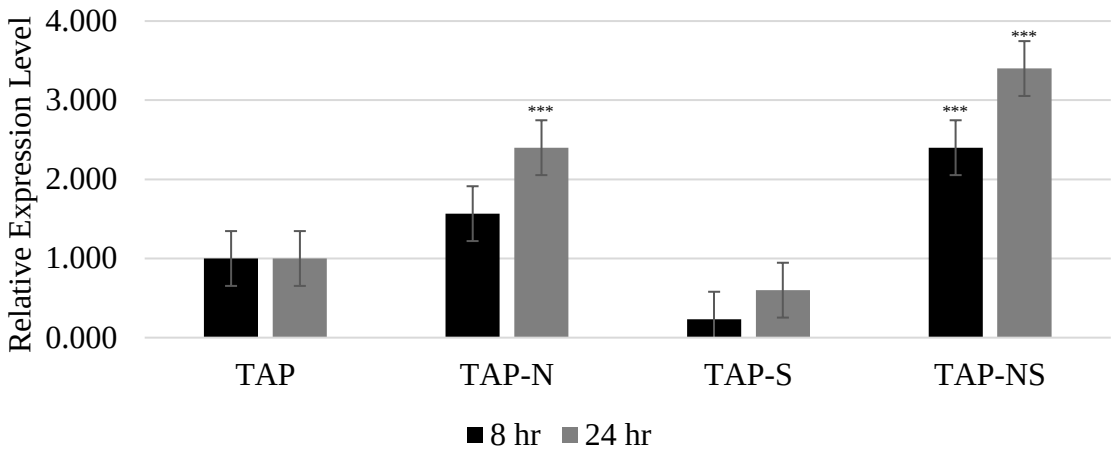

Figure 11. ACCase expression levels at 8 and 24 hr. Fold change was determined using the $2^{-\Delta\Delta Ct}$ method. Expression levels above 1.000, as compared to the TAP control, are considered upregulated; expression levels below 1.000 are considered down regulated. Mean values were determined by three replicates. Bars within treatment, non-overlapping 99% confidence intervals indicate significant difference α= 0.01.

Table 12. Analysis of variance for ACCase expression levels

Source	DF	Type III SS	Mean Square	F Value	Pr > F
Model	10	84.284	8.428	107.679	<0.001
Blk	2	0.437	0.219	2.795	0.095
Trmt	3	21.568	7.189	91.850	<0.001
Time	1	1.815	1.815	23.188	<0.001
Trmt*Time	3	0.928	0.309	3.953	0.031
Error	14	1.096	0.078		

R-Square= 0.987 (Adjusted R-Squared= 0.978)

Expression levels of the ACCase gene were analyzed after being subjected to nutrient deprivations for 8 hr and 24 hr. Acetyl-CoA carboxylase (ACCase) is a key rate-limiting enzyme that catalyzes the first step in the synthesis of fatty acids and plays an important role in fatty-acid synthesis and catabolism (Xu et al., 2018). ACCase can catalyze the first reaction of the fatty acid biosynthetic pathway by converting acetyl CoA and CO_2 into malonyl CoA. After subjecting our cells to 8 hr of N and S deprivation, we found that ACCase expression levels increased two-fold. We observed the same trend in cells subjected to N deprivation; however, cells subjected to S deprivation decreased their expression of ACCase. After 24 hr,

the expression levels of ACCase in both N deprivation and in N and S deprivation increased; and were significantly different from the TAP control (Figure 10).

Xu et al. (2018) studied the role of the ACCase gene under nitrogen deprivation by co-culturing *C. reinhardtii* with a nitrogen-fixing aerobic bacterium, *Azobacter chroococcum*. The expression levels of ACCase expression in the co-culture grown in N deprivation were higher than those in pure *C. reinhardtii*. Although these cells were grown with a nitrogen-fixing bacterium, these cells still exhibited an increased amount of lipids as per FAME analysis that coincided with their increased expression of ACCase (Xu et al., 2018). Whereby, a study by Atikij et al. (2019) treated *C. reinhardtii* cells with 200 mM NaCl. A transcriptional analysis at 0, 6 and 12 hr was conducted. They examined the expression levels of several genes including ACCase. Atikij et al.'s (2019) study found ACCase to be significantly up-regulated (1.87 $\pm$0.05 fold) after 6 hr of stress, and then declined slightly after 12 hr. In a study conducted by Park et al., they found that fatty acid synthesis genes, including ACCase, were significantly upregulated after 6 hr of N deprivation with a maximum expression at 24 hr (2015). These results correlate with the results of our study whereby there was an increase in ACCase expression after 8 hr and 24 hr of stress. The addition of salt and the deprivation of nutrients are both stresses that elicit an increase in lipid biosynthesis (Atikij et al., 2019; Salas-Montantes et al., 2018; Xu et al. 2018). Our results of ACCase gene expression analysis, provide additional evidence that nutrient deprivation can upregulate the expression of genes involved in the fatty acid biosynthesis pathway.

PEPC expression level. RNA isolates were reverse transcribed into cDNA and used for amplification to assess expression levels of PEPC regarding treatments after 8 hr and 24 hr. The average Ct value for actin was 18.0. After normalizing our genes of interest to our housekeeping gene, we found PEPC Ct values in our TAP control to exhibit an average of 22.0 and 25.2 respectively. We observed significant interaction effect between treatments and day ($F_{(3,14)}$=12.303, p<.001) (Table 12). This means that the trend for PEPC expression across four levels of days varies significantly among treatments. Given that there is significant interaction, the emphasis is on the nature of this interaction which is depicted in Figure 11. As compared to

the TAP control, cells subjected to TAP-N decreased in ACCase expression levels after 8hr and increased two-fold after 24 hr. Although not significantly different from the TAP control, cells subjected to TAP-S increased in PEPC expression after 8 hr and 24 hr. Cells subjected to TAP-NS displayed a decrease in PEPC expression after 8 hr, however, this was not significantly different from the TAP control at 8 hr. After 24 hr of N and S deprivation, expression of PEPC increased three-fold as compared to the TAP control. (Figure 10). Thus, the deprivation of both nitrogen and sulfur causes an increase in PEPC expression after 24 hr in cc5373-sta6.

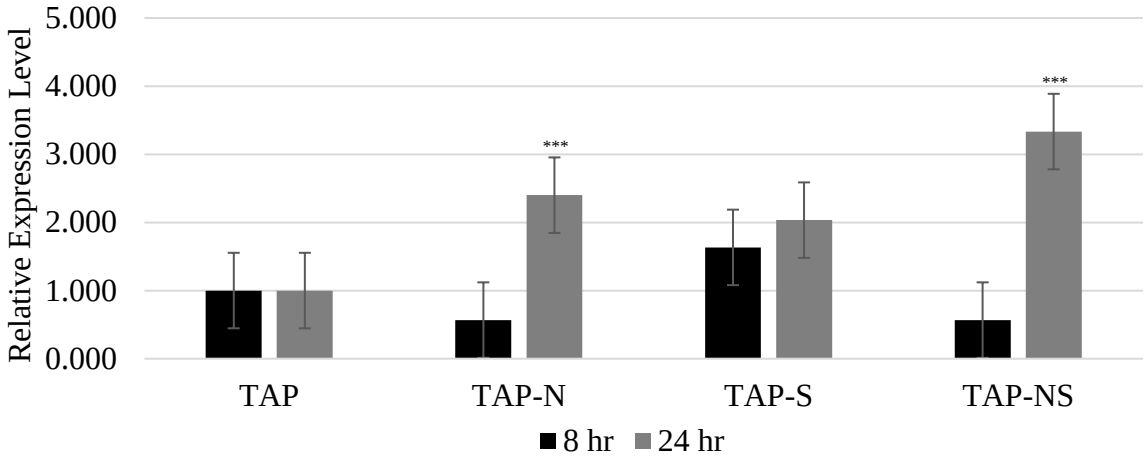

Figure 12. PEPC expression levels at 8 and 24 hr. Fold change was determined using the $2^{-\Delta\Delta Ct}$ method. Expression levels above 1.000, as compared to the TAP control, are considered upregulated; expression levels below 1.000 are considered down regulated. Mean values were determined by three replicates. Bars within treatment, non-overlapping 99% confidence intervals indicate significant difference α= 0.01.

Table 13. Analysis of variance for PEPC expression levels

Source	DF	Type III SS	Mean Square	F Value	Pr > F
Model	10	79.558	7.956	39.743	<0.001
Blk	2	0.611	0.305	1.526	0.252
Trmt	3	3.277	1.092	5.456	0.011
Time	1	9.375	9.375	46.833	<0.001
Trmt*Time	3	7.388	2.463	12.303	<0.001
Error	14	2.802	0.200		

R-Square= 0.966 (Adjusted R-Squared= 0.942)

Phosphoenolpyruvate carboxylase (PEPC) is involved in regulating photosynthesis and respiration, replenishing amino acid metabolism, and catalyzing the formation of oxaloacetate to pyruvate. Thus, PEPC is an initiator of the protein metabolism pathway in *C. reinhardtii* cells and is expected to be expressed constitutively under normal growth conditions. In this study, the levels of expression of PEPC were determined under N and S deprivation conditions after 8 and 24 hr. Our results indicated that after 8 hr of deprivation in both nitrogen deprived treatments (N and NS) PEPC expression decreased as compared to the TAP control (Figure 11). On the other hand, cells subjected to sulfur deprivation for 8 hr displayed an increase in PEPC expression (Figure 11). These findings correlate to the delayed response that cells subjected to sulfur deprivation have as a result of autophagy and recycling cellular components and organelles (Kamalanathan et al., 2016; Cakmak et al., 2012). After 24 hr of N and S deprivation PEPC expression was found to be upregulated. Cells subjected to TAP-N and TAP-S also have upregulated PEPC expression levels in both time intervals (Figure 11).

In the study by Xu et al. (2018), levels of expression of the PEPC gene in N deprivation were assessed at Days 0, 1, 5 and 9. After one day of deprivation, PEPC expression levels were shown to increase in *C. reinhardtii* cells; however, after 5 and 9 days of N deprivation PEPC expression levels decreased significantly. Although our transcriptional analysis was conducted over the course of 8 and 24 hr the increase in expression of PEPC was similar to the results observed after one day of N deprivation in the study by Xu et al. (2018). Subsequent days of nutrient deprivation are known to decrease PEPC expression levels demonstrating that N limitation inhibits the expression of the PEPC gene. Although this study did not report on nutrient deprivation conditions after 24 hr, the effect of nutrient deprivation on PEPC expression levels should be mentioned. The PEPC gene has been known to be manipulated to increase lipid production in *C. reinhardtii*. To further support the effect of inhibition of PEPC on lipid synthesis, a confocal microscopy analysis conducted by Deng et al. demonstrated that a knockout of phosphoenolpyruvate carboxylase isoform 1 (CrPEPC1) increased lipid content by 20-39% after six days of cultivation (2014). Results from this study also demonstrated that mRNA expression of CrPEPC1 decreased by 74-98% indicating the effectiveness of their RNAi silencing constructs (Deng et al., 2014).

Utilizing artificial microRNA technology to inhibit PEPC genes, Wang et al. dramatically increased the total fatty acid content by 29-49% with an increased content of C16-C22 fatty acids (2017). These studies along with ours further support that when PEPC is inhibited, pyruvate will be converted to acetyl-CoA via pyruvate dehydrogenase to facilitate lipid synthesis. Thus, nitrogen can act as a signaling molecule to regulate the expression of specific genes when subjected to nutrient stress (Deng et al., 2014; Wang et al., 2017; Xu et al., 2018). With decreased expression of PEPC, lipid accumulation will increase dramatically especially under nitrogen-deficient conditions.

4 CONCLUSIONS AND RECOMMENDATIONS

In this study, we used *C. reinhardtii* cc5373-sta6, starchless mutant sta6 and cultivated the cells under TAP media that was deprived of both nitrogen and sulfur. This cultivation strategy was utilized to enhance lipid over accumulation in the cells over the course of 0, 2, 4 and 6 days. Cells subjected to nitrogen and sulfur deprivation displayed an increase in cell density and decrease in chlorophyll content conferring to their acclimation and survivability by the observation of increased storage compounds in the form of lipids. Over the course of the six days, it was determined that sta6 cells subjected to nitrogen and sulfur deprivation did over accumulate lipids comparable to that of cells subjected to nitrogen free media and sulfur free media. Levels of expression of genes that regulate lipid metabolism were shown to increase correlating to the increase of lipids observed via confocal microscopy. In summary, cc5373-sta6 cells were able to survive under the nitrogen and sulfur deprivation condition for six days and they were able to enhance their lipid output. This study provides a cultivation strategy for increasing the lipid production of cc5373-sta6 without compromising the cells' integrity.

To give more insight on cc5373-sta6's potential as a source of energy for biofuel production., it would be of use to perform the same assays performed in this study with the wild-type strain, cc-124. The comparison of the wild-type strain and the starchless mutant will provide more evidence on cc5373-sta6's capability of lipid biosynthesis under NS deprivation. To further aid in characterizing cc5373-sta6 under nitrogen and sulfur deprivation, quantitatively determining the lipid content of the algal cells are recommended. A standard lipid content determination assay can be utilized by extracting lipids and weighing out the product every 48 hr (Xu et al., 2018; Atikij et al., 2019). This will further characterize the lipid productivity of the algal cells under stress overtime. The characterization of the type of fatty acid content of cc5373-sta6 under nitrogen and sulfur deprivation especially at two days warrants attention. This will aid in determining if cc5373-sta6 could meet the required fatty acid composition for biodiesel production. Gas chromatography-mass spectrometry (GC-MS), and/or a fatty acid methy ester (FAME) analysis can be conducted to identify and characterize the different types of lipids (Pflaster et al., 2014; Salas-Montantes et al., 2018; Atikij et al., 2019). GC-MS can establish lipid classes, lipid chain length and

degree of desaturation that can impact the potential of cc5373-sta6 as a renewable source for biofuel production. Conducting lipid productivity tests and FAME analysis, will establish the potential energy output from the starchless mutant under a combination of nitrogen and sulfur deprivation. The results of these experiments will provide a basis for the protentional of cc5373-sta6 strain for biofuel production.

5 REFERENCES

Aro EM. (2016) From first generation biofuels to advanced solar biofuels. Ambio. 45, 24-31.

Atikij T, Syaputri Y, Iwahashi H, Praneenararat T, Sirisattha S, Kageyama H, Waditee-Sirisattha R. (2019) Enhanced Lipid Production and Molecular Dynamics under Salinity Stress in Green Microalga Chlamydomonas reinhardtii. Mar Drugs. 17(8), 484.

Ball SG. (1998) Regulation of starch biosynthesis, p. 549–567. *In* J.-D. Rochaix, M. Goldschmidt-Clermont, and S. Merchant (ed.), The molecular biology of chloroplasts and mitochondria in Chlamydomonas. Kluwer Aca-demic Publishers, Dordrecht, Netherlands.

Ball SG. (2002) The intricate pathway of starch biosynthesis and degradation in the monocellular alga *Chlamydomonas reinhardtii*. Aust. J. Chem. 55:49–59.

Ball, S. G., and P. Deschamps. (2009) Starch metabolism, p. 1–40. *In* D. Stern (ed.), The Chlamydomonas sourcebook, 2nd ed. Organellar and metabolic processes, vol. 2. Academic Press, Oxford, United Kingdom.

Blatti JL, Beld J, Behnke CA, Mendez M, Mayfield SP, Burkart MD. (2011) Manipulating fatty acid biosynthesis in microalgae for biofuel through protein-protein interactions. PLos One. 7, e42949.

Cakmak T, Angun P, Demiray Y, Ozkan A, Elibol Z, Tekinay T. (2012) Differential Effects of Nitrogen and Sulfur Deprivation on Growth and Biodiesel Feedstock Production of Chlamydomonas reinhardtii. Biotechnology and Bioengineering. 109(8): 1947-1957.

Cakmak ZE, Plmez TT, Cakmak T, Menemen Y, Tekinay T. (2015) Antioxidant response of Chlamydmonas reinhardtii grown under different element regimes. Phycological Research. doi.org/10.1111/pre.12096

Chen D, Yuan X, Liang L, Liu K, Ye H, Liu Z, Liu Y, Huang L, He W, Chen Y, Zhang Y, Xue T. (2019) Overexpression of acetyl-CoA carboxylase increases fatty acid production in the green alga Chlamydomonas reinhardtii. Biotechnol Lett. 41: 1133-1145.

Chioccioli M, Hankamer B, Ross I. (2014) Flow Cytometry Pulse Width Data Enables Rapid and

Sensitive Estimation of Biomass Dry Weight in the Microalgae Chlamydomonas reinhardtii and Chlorella vulgaris. Plos One. 9(5): 1-12

Chochois V, Dauville D, Beyly A, Tolleter D, Cuine S, Timpano H, Bal S, Cournac L, Peltier G. (2009) Hydrogen production in Chlamydomonas: photosystems II-dependent and -independent pathways differ in their requirement for starch metrabolism. Plant Physiol. 151: 631-640.

Dean AP, Sigee DC, Estrada B, Pittman JK. (2010) Using FTIR spectroscopy for rapid determination of lipid accumulation in response to nitrogen limitation in freshwater microalgae. Bioresour Technol. 101 (12): 4499-4507.

Demirbas A. (2008) Recent progress in bio renewable feedstocks. Energy Edu Sci Technol. 22:69-95.

Deng X, Cai J, Li Y, Fei X. (2014) Expression and knockdown of the PEPC1 gene affect carbon flux in the biosynthesis of triacylglycerols by the green alga Chlamydomonas reinhardtii. Biotechnol Lett. 36:2199-2208.

Devadasu E, Chinthapalli DK, Chouhan N, Madireddi SK, Rasineni GK, Sripadi P, Subramanyam R. (2019) Changes in the photosynthetic apparatus and lipid droplet formation in Chlamydomonas reinhardtii under nitrogen deficiency. Photosynthesis Research. 139: 253-266.

Doan TTY, Sivaloganathan B, Obbard JP. (2011) Screening of marine microalgae for biodiesel feedstock. Biomass Bioenergy. 35:2534-2544.

Erickson P, Lazarus M, Piggot G. (2018) Limiting fossil fuel production as the next big step in climate policy. Nature Climate change. 8:1037-1043

Fufsler TP, Castelfranco PA, Wong YS. (1984) Formation of Mg-Containing chlorophyll precursors from protoporphyrin IX, aminolaevulinic acid, and glutamate in isolated, photosynthetically competent, developing chloroplasts. Plant Physiol. 74(4):928-933.

Gargouri M, Bates PD, Park JJ, Kirchhoff H, Gang DR. (2017) Functional photosystem I maintains proper energy balance during nitrogen depletion in Chlamydmonas reinhardtii, promoting triacylglycerol accumulation. Biotechnol. Biofuels. 10:89.

Goodenough UW, Lin H, Lee JH. (2007) Sex determination in Chlamydomonas. Semin Cell Dev Biol. 18: 350-361.

Goodenough U, Blaby I, Casero D, Gallaher SD, Goodson C, Johnson S, Lee JK, Merchant SS, Pellegrini M, Roth R, Rusch J, Singh M, Umen JG, Weiss TL, Wulan T. (2014) The Path to Triacylglyceride Obesity in the sta6 Strain of Chlamydomonas reinhardtii. American Society for Microbiology. 13(5): 591-613.

Grechanik V, Romanova A, Naydov I, Tsygankov A. (2020) Photoautotrophic cultures of Chlamydomas reinhardtii: sulfur deficiency, anoxia, and hydrogen production. Photosynthesis Research. 143, 275-286.

Hang Lt, Mori K, Tanaka Y, Morikawa M, Toyama T. (2020) Enhanced lipid productivity with combination of NaCl and $CaCl_2$ stresses. Bioprocess and Biosystems Engineering. 43: 971-980.

Hasan H, Abd-Rahim MH, Campell L, Carter D, Abbas A, Montoya A. (2018) Overexpression of acetyl-coa carboxylase in, aspergillus terreus, to increase lovastatin production. New Biotechnol. 44:64.

Jain, V. (2019). Fossil Fuels, GHG Emissions and Clean Energy Development: Asian Giants in a Comparative Perspective. *Millennial Asia*, *10*(1), 1–24.

Kamalanathan M, Pierangelini M, Shearman LA, Gleadow R, Berdall John. (2016) Impacts of nitrogen and phosphorus starvation on the physiology of Chlamydomonas reinhardtii. J Appl Phycol 28: 1509-1520.

Kao PH, Ng IS. (2017) CRISPRi mediated phosphoenolpyruvate carboxylase regulation to enhance the production of lipid in Chlamydomonas reinhardtii. Bioresource Technology. 245, 1527-1537.

Kim JH, Jin HO, Park JA, Chang YH, Hong YJ, Lee JK. (2014) Comparison of three different kits for extraction of high-quality RNA from frozen blood. SpringerPlus. 3:76, 1-5.

Koo KM, Jung S, Lee BS, Kim J, Jo YD, Choi H, Kang S, Chung G, Jeong W, Ahn J. (2017) The Mechanisms of Starch Over-Accumulation in Chlamydomonas reinhardtii High-Starch Mutants Identified by Comparative Transcriptome Analysis. Front Microbiol. 8:858.

La Russa M, Bogen C, Uhmeyer A, Doebbe A, Flippone E, Kruse P, Mussgnug JH. (2012) Functional

analysis of three type-2 DGAT homologue genes for triacylglycerol production in the green microalga Chlamydmonas reinhardtii. J. Biotechnolol. 162, 13-20.

Meng Y, Chen H, Liu J, Zhang CY. (2020) Melatonin facilitates the coordination of cell growth and lipid accumulation in nitrogen-stressed Chlamydomonas reinhardtii for biodiesel production. Algal Research. 46, 101786.

Merchant SS, Kropat J, Liu B, Shaw J, Warakanont J. (2012) TAG, You're it! Chlamydomonas as a reference organism for understanding algal triacylglycerol accumulation. Current Opinion in Biotechnology. 23:352-363.

Moazami N, Ranjbar R, Ashori A, Tangestani M, Nejad A. (2011) Biomass and lipid productivities of marine microalgae isolated from the Persian Gulf and the Qeshm Island. Biomass Bioenergy 35(5):1935–1939.

Moellering ER, Benning C. (2010) RNA interference silencing of a major lipid droplet protein affects lipid droplet size in Chlamydomonas reinhardtii. Eukaryot Cell 9(1):97–106.

Msanne J, Xu D, Konda AR, Casas-Mollano A, Awada T, Cahoon EB, Cerutti H. (2012) Metabolic and gene expression changes triggered by nitrogen deprivation in the photoautotrophically grown microalgae Chlamydmonas reinhardtii and Coccomyxa sp. C-169. Phytochemicstry. 75, 50-59.

Park JJ, Wang H, Gargouri M, Deshpande RR, Skepper JN, Holguin O, Juergens MT, Shachar-Hill Y, Hicks LM, Gang DR. (2015) The response of Chlamydomonas reinhardtii to nitrogen deprivation: s systems biology analysis. The Plant Journal. 81, 611-624.

Perry M, Talbot M, Alberte R. (1981) Photoadaptation in marine phytoplankton: response of the photosynthetic unit. Mar Biol. 62:91-101.

Piggot G, Verkuijl C, van Asselt H, Lazarus M. (2020) Curbing fossil fuel supply to achieve climate goals. Clime Policty. 20(8)881-887.

Pflaster EL, Schwabe MJ, Becker J, Wilkinson MS, Parmer A, Clemente TE, Cahoon EB, Riekhof WR.

(2014) A High-Thoroughput Fatty Acid Profiling Screen Reveals Novel Variations in Fatty Acid Biosynthesis in Chlamydomonas reinhardtii and Related Algae. Eukaryotic Cell. 13(11) 1431-1438.

Potijun S, Jaingam S, Sanevas N, Vajrodaya S, Sirikhachornkit A. (2020) Improving the co-production of triacylglycerol and isoprenoids in Chlamydomonas. Biofuel Research Journal. 28. 1235-1244.

Raman R, Kim B, Cho D, Ko S, Oh H, Kim H. (2013) Lipid droplet synthesis is limited by acetate availability in starchless mutant of Chlamydomonas reinhardtii. FEBES Letters. 587. 370-377.

Rasala BA, Mayfield SP. (2014) Photosynthetic biomanufacturing in green algae; production of recombinant proteins for industrial, nutritional, and medical uses. Photosynth. Res. 123, 227-239.

Rengel R, Smith R, Haslam R, Sayanova O, Vila M, Leon R. (2018) Overexpression of acetyl-CoA synthetase (ACS) enhances the biosynthesis of neutral lipids and starch in the green microalga Chlamydomonas reinhardtii. Algal Research. 31: 183-193.

Rodionova MV, Poudyal RS, Tiwari I, Voloshin RA, Zharmukhamedov SK, Nam HG, Allakhverdiev SI. (2017) Biofuel production: Challenges and opportunities. International Journal of Hydrogen Energy. 42(12): 8450-8461.

Salas-Montantes CJ, Gonzalez-Ortega O, Ochoa-Alfaro AE, Camarena-Rangel R, Paz-Maldonado LMT, Rosales-Mendoza S, Rocha-Uribe A, Soria-Guerra RE. (2018) Lipid accumulation during nitrogen and sulfur starvation in Chlamydomonas reinhardtii overexpressing a transcription factor. J Applied Phycology. 30:1721-1733.

Sathe S, Orellana MV, Baliga NS, Durand PM. (2019) Temporal and metabolic overlap between lipid accumulation and programed cell death due to nitrogen starvation in the unicellular chlorophyte Chlamydomonas reinhardtii. Phychological Research. 67(3): 173-83.

Scranton MA, Ostrand JT, Fields FJ, Mayfield SP. (2015) Chlamydomonas as a model for biofuels and bio-products production. The Plant Journal. 82, 523-531.

Schmollinger S, Muhlhaus T, Boyle NR, Blaby IK, Casero D, Mettler T, Mosely JL, Kropat J, Sommer F,

STrenkert D, Hemme D, Pellegrini M, Grossman AR, Stitt M, Schroda M, Merchant SS. (2014) Nitrogen-Sparing Mechanisms in Chlamydomonas Affect the Transcriptome, the Proteome, and Photosynthetic Metabolism. The Plant Cell. 26, 1410-1435.

Shin YS, Choi H, Choi, JW, Lee JS, Sung YJ, Sim SJ. (2018) Multilateral approach on enhancing economic viability of lipid production from microalgae: a review. Bioresource Technology. 335-344.

Sierra LS, Dixon CK, Wilken LR. (2017) Enzymatic cell disruption of the microalgae Chlamydomonas reinhardtii for lipid and protein extraction. *Algal Research*. 149-159.

Smith KR, Frumkin H, Balakrishnan K, Butler CD, Chafe ZA, Fairlie I, Schneider M. (2013) Energy and Human Health. *Annual Review of Public Health*, *34*(1), 159–188.

Song D, Xi B, Sun J. (2016) Characterization of the Growth, Chlorophyll Content and Lipid Accumulation in a Marine Microalgae Dunaliella tertiolecta under Different Nitrogen to Phosphorous Ratios. J Ocean Univ China. (1): 124-130.

Sung YJ, Choi HI, Lee JS, Hong ME, Sim SJ. (2019) Screening of oleaginous algal strains from Chlamydomonas reinhardtii mutant libraires via density gradient centrifugation. Biotechnology and Bioengineering. 116 (12): 3179-3188.

Tran QG, Kichul C, Park SB, Kim R, Lee YJ, Kim HS. (2019) Impairment of starch biosynthesis results in elevated oxidative stress and autophagy activity in Chlamydomonas reinhardtii. Sci Rep. 9,9856.

Trentacoste EM, Shrestha RP, Smith SR, Gle C, Hartmann AC, Hildebrand M, Gerwick WH. (2013) Metabolic engineering of lipid catabolism increases microalgal lipid accumulation without compromising growth. Proceedings of the National Academy of Sciences U.S.A. 110: 19748-19753.

Tsygankov A, Abdullatypov AV. (2016) Hydrogen metabolism in microalgae. Scrivenger Publishing LLC, Salem. 133-161.

Valledor L, Escandon M, Meijon M, Nukarinen E, Canal MJ, Weckwerth W. (2014). A universal protocol

for the combined isolation of metabolites, DNA, long RNAs, small RNAs, and proteins from plants and microorganisms. 79, 173-180.

Wang C, Chen X, Li H, Wang J, Hu, Z. (2017) Artifical miRNA inhibiton of phosphoenolpyruvate carboxylase increases fatty acid production in a green microalga Chlamydomonas reinhardtii. Biotechnology for Biofuels. 10, 91.

Wang ST, Ullrich N, Joos S, Waffenschmidt S, Goodenough U. (2009) Algal lipid bodies: Stress induction, purification, and biochemical characterization in wild-type and starchless Chlamydomonas reinhardtii. Eukaryotic Cell. 8(12), 1856-1868.

Willfinger WW, Mackey K, Chomczynski P. (1997) Effect of pH and Ionic Strength on the Spectrophotometric Assessment of Nucleic Acid Purity. Biotechniques. 22 (3): 474-481.

Work V, Radakovits R, Jinkerson R, Meuser J, Elliott L, Vinyard D, Laurens L, Dismukes G, Posewitz M. (2010). Increase Lipid Accumulation in the Chlamydomonas reinhardtii sta7-10 Starchless Isoamylase Mutant and Increased Carbohydrate Synthesis in complemented Strains. Eukaryotic Cell. 9(8): 1251-1261.

Wuebbles DJ, Jain AK. (2001) Concerns about climate change and the role of fossil fuel use. *Fuel Processing Technology*, *71*(1–3), 99–119.

Xu F & Pan J. (2020) Potassium channel KCN11 is required for maintaining cellular osmolarity during nitrogen starvation to control proper cell physiology and TAG accumulation in Chlamydomonas reinhardtii. Biotechnol Biofuels. 13: 129.

Xu L, Cheng X, Wang Q. (2018) Enhanced Lipid Production in Chlamydomonas reinhardtii by Co-Culturing with Azotobacter chroococcum. Frontiers in Plant Science. 9: 1-13.

Xu L, Fan J, Wang Q. (2019) Omics Application of Bio-Hydrogen Production Through Green Alga Chlamydomonas reinhardtii. Front. Bioeng. Biotechnol. 7: 1-9.

Zabawinski C, Van Den Koornhuyse N, D'Hulst C, Schlichting R, Giersch C, Delrue B, Lacroix JM, Preiss J, Ball S. (2001) Starchless mutants of Chlamydomonas reinhardtii lack the small subunit of a heterotetrametric ADP-glucose pyrophosphorylase. Journal of Bacteriology. 183(3): 1069-

1077.

Zhang J, Mueller B, Tyre K, Hersh H, Bai F, Hu Y, Resende M, Rathinasabapathi B, Settles A. (2020) Competitive Growth Assay of Mutagenzied Chlamydomonas reinhardtii Compatible with the International Space Station Veggie Plant Growth Chamber. Frontiers in Plant Science. 11: 1-14.

Zhu Z, Cao H, Li X, Rong J, Cao X, Tian J. (2021) A Carbon Fixation Enhanced Chlamydomonas reinhardtii Strain for Achieving the Double-Win Between Growth and Biofuel Production Under Non-Stressed Conditions. Frontiers in Bioengineering and Biotechnology. 8: 603513.

6 VITA

Name:	David Gonzalez
Email Address:	david.gonzalez@dusty.tamiu.edu
Education:	B.A., Acting, American Musical and Dramatic Academy, 2013
	B.S., Biology, Texas A&M International University, 2019
Publications:	Cavazos P, Gonzalez D, Lanorio J, Ynalvez, R. 2021. Secondary metabolites, antibacterial and antioxidant properties of the leaf extracts of *Acacia rigidula* benth. and *Acacia berlandieri* benth. *SN Applied Science.* 3:522, 1-14